FCTUC DEPARTAMENTO DE ENGENHARIA CIVIL
FACULDADE DE CIÊNCIAS E TECNOLOGIA
UNIVERSIDADE DE COIMBRA

Perforation effect in the bearing capacity of shallow foundations

Dissertação apresentada para a obtenção do grau de Mestre em Engenharia Civil na Especialidade de Geotecnia

Author

Vera Lúcia Nora Fidalgo Matias

Advisors

Paulo Miguel Cunha Matos Lopes Pinto

Jérémy de Barbarin

Coimbra, fevereiro, 2016

ACKNOWLEDGEMENTS

I would like to express my gratitude to my supervisor, Professor Paulo Miguel Cunha Matos Lopes Pinto. His support, expertise guidance, understanding and his incredible patience, made this work possible. I am thankful for his sharing of knowledge and for being a source of motivation. It was a great pleasure to work with him.

I am hugely grateful to Subsea 7, in particular to Jérémy de Barbarin, Régis Wallerand and Mersina Cafi, for the opportunity to collaborate with them and develop a topic with a great interest.

I feel a distinct sense of gratitude to all my friends and colleagues that accompanied me during the unforgettable college years, for their friendship. During all these years, we dreamed, laughed, believed… shared incredible moments, always with a word of support, encouragement and faith for each other. I'll keep each one of them in my heart.

I would also like to thank to those that are not my close friends or family, but are present in my life and really make all the difference to me.

Finally, to my parents, Vítor and Helena, and my brother, Tomás, and to all my closest family, in particular my cousin Ivo, a huge thank you. Since I was born, these are those who are always there, with love, right by my side, in each step, in each struggle, in each success. These are those that really inspire me and are my motivation to always be better.

A heartfelt THANK YOU!

"We must find time to stop and thank the people who make a difference in our lives."
John F. Kennedy

ABSTRACT

With the Oil & Gas industry crisis, installation companies as Subsea 7 have to focus more than ever in efficiency and quality of their services. Installation of structures takes a big role in projects, not just because it is the critical phase where the company delivers the product but also because it can condition the design of the product itself.

While the industry goes forward, new challenges are found and new engineering solutions need to be developed. Nowadays, deep water field exploration is becoming more common (up to 3500 m water depth). Hence, oil companies are rather keen on having all the field development subsea than having the structures at surface. Geotechnical Engineer plays a big role in the development and improvement of efficient foundation solutions needed in these field architectures. The geological properties of the seabed under deep water are commonly very poor (e.g. soft clays) which creates difficulties during the structures foundations design phase. In addition, during design phase geotechnical engineers are limited by the capabilities of the installation vessels (e.g. crane capacity, deck space).One of the proposed solutions for the optimization of shallow foundations is to insert small perforations to reduce de forces applied to the structure and transmitted to the crane during the installation process. However, this solution also has its disadvantages.

The present dissertation analyses the effect of perforation on shallow foundations, known as mudmats, for offshore structures during design life. Assesses and compares different perforation configuration, using a ratio between 30 and 40% of the foundation footprint, since it is the minimum perforation ratio needed to reduce the hydrodynamic loads. Moreover, analysis for skirted foundations are also performed.

The study was conducted using 3D finite element models, using Rocscience computer program *RS3*. The main conclusions were that the holes' shape has small influence on the foundation bearing capacity; foundations with a greater number of holes tend to have higher bearing capacity; the perforation ratio for some cases can be increased up to about 40% without affecting the foundation capacity.

Keywords: Geotechnical Engineering | Mudmat | Offshore | Perforation | Perforated Foundations

RESUMO

Com a crescente crise na indústria de petróleo e gás, as empresas responsáveis pelo dimensionamento e instalação das estruturas de extração e exploração destes recursos, como a Subsea 7, têm que estar focadas cada vez mais na eficiência e qualidade dos seus serviços. A instalação das estruturas representa um papel importante nos projetos, não só porque constitui a fase crucial em que o produto é entregue mas também porque condiciona o dimensionamento da própria estrutura.

À medida que a indústria cresce, surgem novos desafios obrigando a engenharia a desenvolver novas soluções. Atualmente, a exploração em águas profundas é cada vez mais comum, atingindo já profundidades superiores a 3500 metros. Por estas razões, aumenta o interesse das empresas petrolíferas em ter todos os equipamentos de exploração submersos, ao invés estruturas maioritariamente superficiais. No entanto, no fundo do oceano, os solos presentes são geralmente pouco competentes, tendo propriedades mecânicas bastante baixas, criando algumas dificuldades no dimensionamento das fundações das estruturas. Além disso, também nesta fase, devem ser tida em conta a capacidade dos navios de instalação das estruturas (por exemplo, a capacidade das gruas, espaço nas plataformas). Uma das soluções desenvolvidas para otimizar as fundações superficiais é a introdução de pequenos orifícios de forma a aliviar as forças aplicadas na estrutura e induzidas nas gruas na fase de instalação, sobretudo forças hidrodinâmicas. Contudo, esta solução tem também as suas desvantagens.

A presente dissertação analisa o efeito da perfuração na capacidade de carga de fundações superficiais, denominadas *mudmats*, para estruturas *offshore* durante o seu ciclo de vida. Avalia e compara também diferentes configurações de perfuração, usando uma área perfurada de cerca de 30 a 40 % da *mudmat*, uma vez que é a percentagem mínima necessária para reduzir as forças hidrodinâmicas. De forma complementar, são analisados também estes efeitos aplicados a fundações reforçadas com saias.

O estudo foi realizado usando modelos de elementos finitos tridimensionais, com recurso programa de cálculo da *Rocscience*, *RS3*. As principais conclusões a salientar são a pouca influência na capacidade de carga das fundações devido à forma dos furos, a maior capacidade de fundações que apresentam maior número de perfurações e, em alguns casos, a percentagem de perfuração pode atingir valores na ordem dos 40% sem afetar o desempenho da fundação.

Palavras-chave: Engenharia Geotécnica | Fundações Perfuradas | Mudmat | Offshore | Perfuração

TABLE OF CONTENTS

LIST OF FIGURES

LIST OF TABLES

SYMBOLOGY

Latin Alphabet

A	Foundation area
A'	Effective area of foundation
B	Width of foundation
B'	Effective width of foundation
C_c	Compression index
C_α	Secondary compression index
c'	Cohesion intercept of Mohr-Coulomb failure envelope in terms of effective stress at failure
c_v	Coefficient of consolidation
D	Depth of the foundation
d	Skirt's length or Maximum drainage distance
d_{ca}	Depth correction factor
E	Young's Modulus; modulus of elasticity
E_u	Undrained Young's Modulus
e	Eccentricity
e_0	Initial void ratio; voids ratio before primary consolidation
e_1	Void ratio before secondary consolidation
F	Correction factor
F_H	Horizontal force
F_{H1}	Horizontal force on the effective area
F_V	Vertical force
FS	Safety factor
H	Sliding capacity
H_0	Thickness of the consolidated layer
i_{ca}	Load inclination correction factor
k	Rate of increase with depth of the undrained shear strength
L	Length of foundation
N_c	Bearing capacity factor
M	Moment
OCR	Overconsolidation ratio
Q_u	Ultimate bearing capacity resultant
q	Uniform load

q_u	Ultimate bearing capacity
R_{HO}	Sliding resistance on area outside effective area
R_{HP}	Resistance due to horizontal soil pressure on embedded members
s_{ca}	Shape correction factor
s_{cv}	Shape correction factor for circular foundations
s_u	Undrained shear strength
s_{u0}	Undrained shear strength at the top of the layer
T_v	Time factor for one-dimensional consolidation
t	Time at the end of primary consolidation
t_1	Time at the beginning of the period of secondary consolidation in analysis
t_2	Time at the end of the period of secondary consolidation in analysis
U	Average degree of consolidation
u_h	Immediate horizontal displacement
u_v	Short term settlement
$u_{v,pc}$	Settlement due to primary consolidation
$u_{v,sc}$	Settlement due to secondary consolidation

Greek Alphabet

γ	Total unit weight
γ'	Submerged unit weight
γ_{sat}	Unit weight in saturated state
ε	Strain
ε^e	Elastic Strain
ε^p	Plastic Strain
ν	Poisson's ratio
σ'	Effective normal stress
σ'_p	Preconsolidation pressure
σ'_{vf}	Final effective vertical stress
σ'_1	Effective major principal stress
σ'_3	Effective minor principal stress
σ'_f	Effective stress at failure
σ_t	Tensile Strength
τ	Shear stress
τ_f	Shear stress at failure
ϕ	Friction angle; angle of shearing resistance
ψ	Dilatancy angle

ABBREVIATIONS

API	American Petroleum Institute
DNV	Det Norske Veritas
ILT	In-Line Tee
ISO	International Organization for Standardization
LRFD	Load and Resistance Factor Design
PLEM	Pipeline End Manifold
PLET	Pipeline End Termination
SLS	Serviceability Limit State
SUTA	Subsea Umbilical Termination Assembly
ULS	Ultimate Limit State
WSD	Working Stress Design

1 INTRODUCTION

1.1 Introductory Note

In recent years there has been a stimulation on the exploration of natural energy resources in offshore areas.

Offshore holding structures use many types of foundations. Its use is determined by the equipment to support and the type of soil present at the installation site. It can be grouped into two distinct groups: deep foundations and shallow foundations.

The first takes advantage over the shallow foundations when the first layer of soil is very soft clay or there is a high horizontal force applied to the structures. However, the shallow foundations become an alternative in situations where the soil is composed of overconsolidated clays or very dense sands with high bearing capacity. Moreover, the installation of the deep foundation can become unfeasible due to soil density (Randolph and Gourvenec, 2011).

Over time, this type of solution has been improved and applied to many other situations, such as to support wind mills or production line end termination. Shallow foundation can be classified according to three main groups (Bell, 1991), as shown in Figure 1.1:

i) gravity concrete bases - the action of the forces is opposed by the action of the foundation weight;

ii) spudcans - have the particularity of having a jag that enters the soil and increases the sliding resistance;

iii) mudmats - generally consist on a thin plate reinforced with transversal stiffeners, which allows stresses to be transmitted in a more distributed way to the ground.

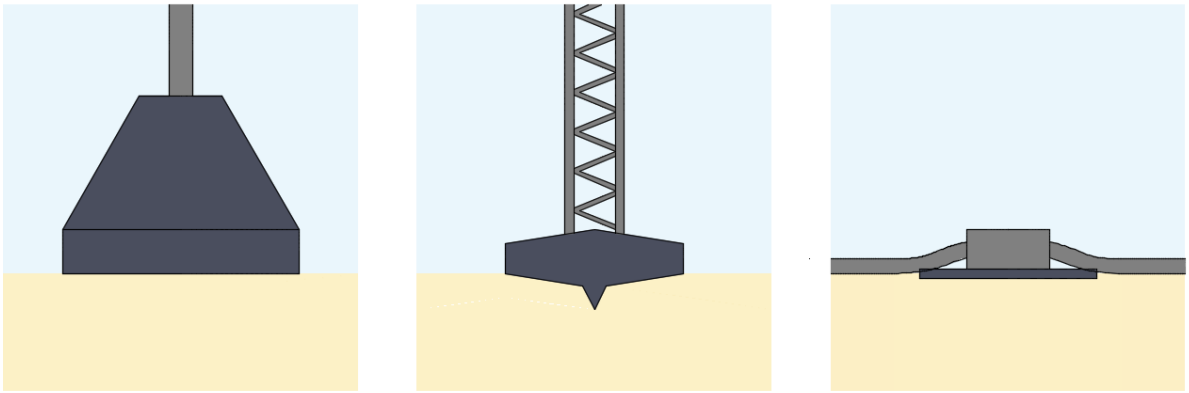

(a) (b) (c)

Figure 1.1 - Shallow foundations for offshore structures: (a) gravity base; (b) spudcan; (c) mudmat

Within this document it is only addressed the perforation effect in mudmats since this type of foundation is the most used for subsea structures (e.g. Pipeline End Terminations and In-Line Tees). These structures are usually quite heavy which makes the soil bearing capacity one of the critical parameter during the design phase.

Commonly, due to the very low shear strength of soils beneath the structures, mudmats need to have a large footprint in order to reduce the settlements and transmit the forces uniformly to the soil, since it has to support not just the dead weight of the structure but also the dynamic forces (e.g. expansion due to thermal variations) during structure's life.

Besides the geotechnical factor, mudmats are often installed at more than 1000 m water depths, making installation a delicate process. During its deployment phases: crossing the splash zone, through the water column and landing phase, structures are subject to high hydrodynamic forces that put into question their integrity.

Thus, perforation in mudmats emerged as a solution to relieve the structure from hydrodynamic forces, making the installation process easier and faster. However, this solution has consequences on the mudmat bearing capacity, which need to be analysed.

1.2 Objective and Methodology

The aim of the present dissertation is to analyse the effects caused by the perforation on mudmats bearing capacity, for perforation ratios between 30 and 40% of the total area. It is expectable to have some conclusions about the reduction of the bearing capacity since these perforation ratios are very high and are not present within the common offshore design standards.

On a first instance, the study will be performed using a regular mudmat with no skirts. Secondly, skirts will be introduced in order to strengthen the vertical bearing capacity, the resistance against sliding and reduce the settlement.

In order to achieve this, different configurations and perforations are studied for a mudmat and both vertical (bearing capacity) and lateral (sliding) resistances are analysed.

The soil profile used in the present study will be the same to the several analyses.

The research will be carried out using numerical modelling with a 3D elasto-plastic finite element program.

1.3 Structure of the document

The document starts with an introductory chapter presenting the scope of work, purpose and a brief description.

Chapter 2, presents a theoretical review carried out to introduce the concepts used within the work. It describes the forces acting on the structure; the soil behaviour theory, potential failure mechanisms and analytical design checks. It also includes conclusions that several authors achieved during similar studies.

Chapter 3 describes in detail the three dimensional model used in the finite element software, explaining and justifying all the configuration chosen. This phase is fundamental to understand how the model behaves and if it represents as accurately as possible the reality; (testing and setting phase of the model).

Chapter 4 presents the results from the analyses, and the first conclusions about the behaviour of this type of footings are derived.

Within Chapter 5, the final conclusions are presented. Within this chapter it is also summarized the work and proposed studies to be undertaken in the future.

2 THEORETICAL BACKGROUND

2.1 Soil Profile

Soil conditions are always a substantial issue when it comes to design a foundation. From the moment the foundation is installed until it is removed, the behaviour of soil can be different depending on its profile, conditioning the foundation design. Therefore, geotechnical surveys take a big role on conception of offshore structures.

The primary method used in offshore site investigations is to collect samples that are afterward tested in laboratories onshore, but it may also include *in situ* tests.

In general, at deep water the seabed is a composition of very soft clays or highly plastic silts. The prospection results typically show normally consolidated soils, with high voids ratios and very poor strength profiles: around 1 kPa at the surface, increasing linearly in depth (Randolph and Gourvenec, 2011, and White et. al., 2005).

Taking into consideration these parameters, subsea construction becomes a challenge, triggering the need to design innovative subsea architectures.

2.2 Mudmats

Installed on seabed, there are structures linked along a pipeline which are generally too heavy, exceeding the capacity of the soil beneath them. In those cases, it is required an additional support, which can be provided by mudmats. The most common structures used within the oil and gas, which require the use mudmats are (TECH-FAB@, 2015):

- Pipeline End Terminations (PLETs);
- Pipeline End Manifolds (PLEMs);
- In-Line Tees (ILTs);
- Subsea Umbilical Termination Assemblies (SUTAs).

Mudmat is a type of shallow foundation. Commonly it consists on a thin steel top plate (carbon steel) reinforced with transversal stiffeners and whose function is to transfer the loads to the soil with contact stresses low enough to warrant the desired safety level. Figure 2.1 presents a basic example of a mudmat and the general stiffeners arrangement. Usually, mudmats have a big footprint that act not just as support to the equipment but also to redistribute the stresses

and reduce the settlements to tolerable values. As other types of shallow foundations a mudmat takes advantage of the resistance mobilised along the failure surface.

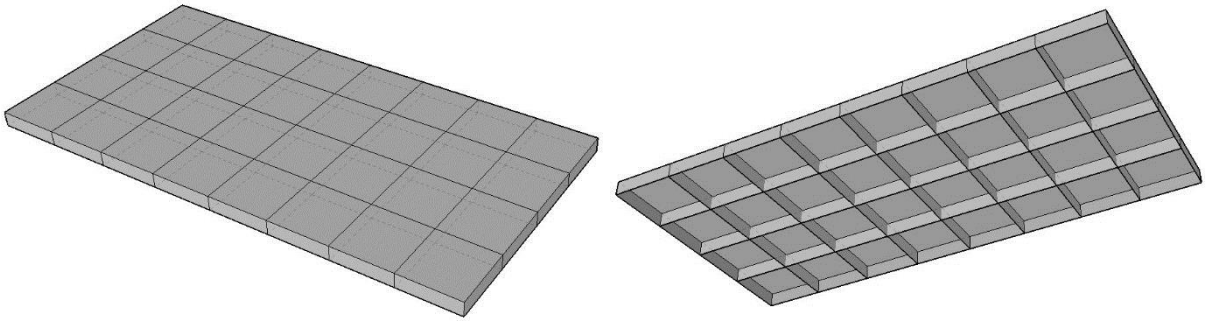

Figure 2.1 – Basic design of a mudmat

2.3 Skirts

Skirted foundations are regular mudmats with vertical thin elements arranged around and/or in its interior, as extended walls.

In a skirted foundation the loads are transferred to deeper soil layers, which typically have higher shear strength. That fact allows a better control of the failure surface, that develops deeper and to soil with higher values of shear strength, which returns in a higher bearing capacity. As a result, it also affects the settlements since the stresses spread along it to deeper layers. In addition, confining the underlying soil, skirts help to resist to slide, generating a soil resistance when submitted to horizontal actions.

Based on the ideas presented above, several studies have been conducted over the years in order to understand the foundations behaviour including structural skirts. Those studies, mainly through experimental testing in sands, assessed the impact on the foundation capacity by playing/varying multiple parameters such as: distance of the skirts to the foundation centre; length; skirt inclination; and load eccentricity.

Pusadkar and Bhatkar (2013) have tried to understand the failure pattern of these footings. The effect of adding skirts to foundations was evaluated using finite element analyses in plane strain-stress conditions. The investigation concluded that the bearing capacity is improved and increased with skirt depth. But regarding settlements, its reduction only happens for two sided skirts (skirts in both sides of the mudmat); one sided skirt (skirt only in one side of the mudmat) mudmats have an increase in settlements, which may be due to sliding. Moreover, the increase of skirts length has been proven to reduce the foundation settlements (e.g. Alves (2014) by laboratory tests and Silva (2014) through numerical analyses).

Furthermore, the use of skirts help on avoiding the corrosion caused by the water flow, currents, and on stabilizing the structures at the seabed.

2.4 Perforation

The most critical phase of a mudmat is the installation. During this process the structure is subjected to hydrodynamic forces which can damage it. And as soon as the structure is fully submerged the added mass, which corresponds to the effect caused by the water acting on the structure, is developed and can become a concern to the integrity of the equipment used for the operation.

Thereby, perforated mudmat emerged as a solution to reduce the forces during de deployment of the structure. The foundation self-weight also decreases, which makes its decommissioning easier, and allows the use of equipment with less capacity. On the other hand, perforation reduces the mudmat effective area affecting its bearing capacity.

Experimental investigations were carried out by White et. al. (2005) in order to assess the impact of perforation size in the embedment and mudmats vertical bearing capacity. The study was performed using a large-scale tank with clayey soil collected at under deep water, equipped with drainage and a 600mm gravel layer at bottom and two layers of geotextile between the gravel and the test soil layers guaranteeing the soil didn't escape during the tests. Above the clay layer a freeboard of water was maintained. Square mudmats were installed vertically at a constant velocity of 2 mm/s, down to a depth of 40% of the mudmat width and held one hour at this point before being removed at the same velocity. Tested mudmats were made from aluminium alloy and had distinct characteristics, varying the width, the holes' shape (square and circular) and/or the holes configuration. Throughout the test, the applied load and displacements were recorded and then correlated to the vertical bearing capacity factor N_c, leading to the conclusion that as the perforation ratio increases:

- the installation resistance decreases;
- the failure mechanisms develops at lower depths;
- the pull out resistance reduces (more dependent on effective width of each grillage element than on perforation ratio).

In addition White et. al. (2005) concluded that an optimal mudmat design would be a large number of small perforations uniformly arranged, as it minimizes the effective width of each grillage element, bearing in mind that in vertically heterogeneous conditions lower effective widths lead to shallower failure mechanisms.

A few years later, Fagundes et al. (2012) conducted an experimental study using a new approach on which a similar test was performed placing it inside a centrifuge. The models consisted in a

clayey soil with the undrained shear strength profile increasing with depth. On the soil's surface, mudmats were installed with two different area ratios. The study allowed to conclude that the higher perforation ratio the smaller the installation resistance. Moreover, the soil plugging tends to increase as the holes diameter become smaller. It was also noticed that to ease the installation process without affecting the bearing capacity the perforation ratios should be less than 10%.

The two references above were crucial to have general conclusions about the impact of perforation in mudmats on soft clayey soils. To add more relevant information and strength the conclusion on this topic it is found important to conduct complementary numerical studies.

2.5 Acting Forces

During all of the installation process, the mudmat is subject to various loads, static and dynamic, which have to be considered at the design phase. This process is complex and needs to be carefully analysed.

The installation process is defined by 3 phases which the structure moves through and the loads vary at each phase:

- In air;
- Splash zone;
- Subsea (fully submerged).

All the process begins on a vessel or cargo barge, with a crane lifting the structure in air, to start the deployment. At this moment the vessel crane supports mainly the structure death weight amplified by motion of the vessel (dynamic amplification). As soon as the structures slams in the water there are additional loads applied that must be accounted for. The waves start slamming into the mudmat causing an oscillation of the structure, which generates high load peaks at the crane tip that can lead to the failure of the equipment. As it goes down, the waves impact decreases becoming null, but there is still the vessel motions inducing a dynamic effect. Additionally the added mass is fully developed and there still are hydrodynamic forces, such as drag forces to account for.

The design life for this structure is typically around 20 years. During this period geotechnical engineers involved on its design must ensure that a soil rupture will not occur. Therefore, the engineers need to consider the forces applied in the structure when it is laid on the seabed (e.g. submerged weight, expansion due to the temperature of the fluids transported, the combination of currents and waves at seabed depth – negligible after 100 meters depth).

When the exploration ends, equipments are removed and some can be reused in other fields. But, to remove an equipment from the seabed it requires to study the conditions of the soil on

which the structure is laid on and the better method to pull it out without damaging the structure nor the vessel equipment within the operation. At this phase, soil has a big influence, not only because of the deposits weight brought by currents but also the interaction between the soil and the structure caused by its adhesion. Hence, the pull out resistance may vary from site to site, mudmat to mudmat, and so as the force needed to be applied by the crane/winch. Furthermore, while the structure crosses the water column downward, hydrodynamic forces will be acting.

During mudmat design only the *in situ* loads are considered, although the installation process can dictate maximum dimensions and weight for the structure in order to keep the loads within the vessel equipment limits.

2.6 Stability of the foundation

The stability of foundations is determined by limit states. It means that it must be ensured the soil can resist to the applied forces without developing a failure mechanism. Moreover, no excessive settlements may occur, ensuring the serviceability during the structure design life. These are known as Ultimate Limit State of bearing capacity and Serviceability Limit State of excessive settlement, respectively.

Ultimate Limit State (ULS) of bearing capacity is reached when the load is higher than what the foundation soil can support and it starts to develop a failure surface, causing large displacements of the foundation.

On the other hand, Serviceability Limit State (SLS) prescribes a limit to the settlements and displacements that the structure can undertake without affecting its normal service conditions.

In terms of design, the ULS are taken as basis, once they are the most critical. Depending on the loads, the soil parameters, the equipment dimensions, among others, several failure surfaces may occur in the ground which must be analysed.

In accordance with DNV CN 30.4 (1992), the main failure mechanisms, illustrated in Figure 2.2, to be considered are:

a) Sliding along base of skirt tip;
b) Sliding along soft layer below skirt tip;
c) Sliding at base with local failure around skirt tips;
d) Conventional deep-seated bearing failure;
e) Deep-seated failures governed by moment equilibrium with centre of rotation above or
f) Below the foundation base.

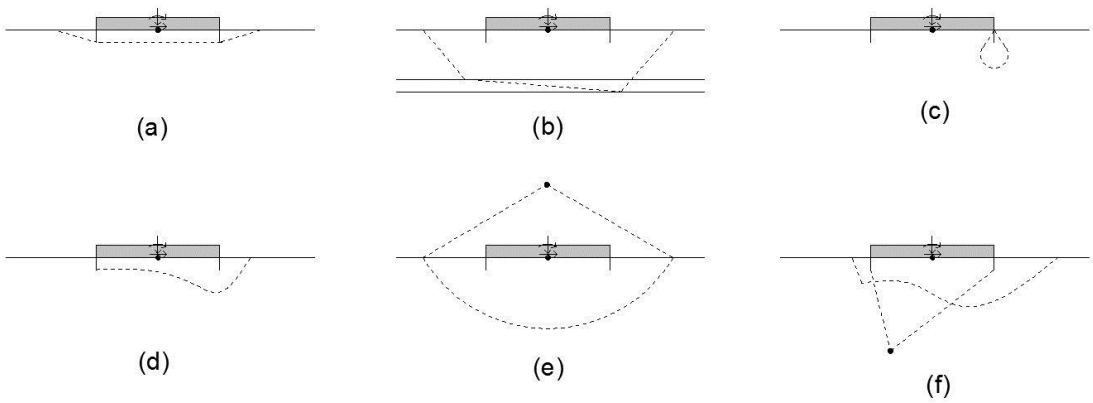

Figure 2.2 – Possible failure mechanisms, adapted from DNV CN 30.4 (1992): (a) sliding at skirt tips; (b) sliding along soft layer; (c) local failure along skirts; (d) deep-seated bearing capacity failure; (e) moment equilibrium centre located anywhere; (f) moment equilibrium centre below foundation base.

The present document studies the bearing and sliding capacity of the mudmat in order to control the development of the failures mechanisms mentioned above.

2.6.1 Bearing Capacity

The principle of bearing capacity relates the vertical and horizontal loads and moment with the footprint of the mudmat, depending on the mechanical properties of the soil and on the foundation geometry and roughness. The vertical force increases until the soil beneath can't further bear and thus, it is defined by the vertical force at the time the soil rupture.

Onshore and offshore fields present very different conditions, such as, the loading that is extremely exigent at sea bottom, the installation process, the conservation and the maintenance or repair operations. These differences contributed to the creation of distinct regulations for each situation. However, in terms of geotechnical requirements, the fundamental principles of stability and displacements are the same. Thus, also the recommended practice establishes the use of the same normative and equations for either situation.

Current practices are based on Terzaghi theory, proposed in 1943, which uses the plasticity theory. Throughout the years, several authors studied his theory and made some adjustments in order to extend his conclusions to other situations. In 1963, Meyerhof developed the equation considered by several authors as the general bearing capacity equation (Dean, 2010). Shape and depth of the mudmat as well as the load inclination are considered by correction factors.

In order to evaluate the foundation bearing capacity as soon as the equipment will be installed on the seabed, it is necessary to perform analyses with undrained conditions. Consequently, the

only soil parameter to consider is the undrained shear strength, since the undrained friction angle of clayey soils is null.

Several normative documents, such as DNV CN 30.4 (1992), ISO 19901-4 (2003), API RP 2A WSD (2005), suggest expressions to calculate the bearing capacity of shallow foundations. To take in account the shear strength increasing linearly with depth DNV CN 30.4 (1992) establishes the following expression:

$$q_u = F\left(N_c\, s_{u_0} + \frac{k\, B'}{4}\right)(1 + s_{ca} + d_{ca} - i_{ca}) \tag{1}$$

where F is a correction factor given in function of the heterogeneity factor kB'/s_{u_0}, that can be seen in Figure 2.3 for rough and smooth footings, where k is the rate of increase with depth of undrained shear strength, B' is the effective width of foundation and s_{u_0} is the undrained shear strength at the top of the layer.

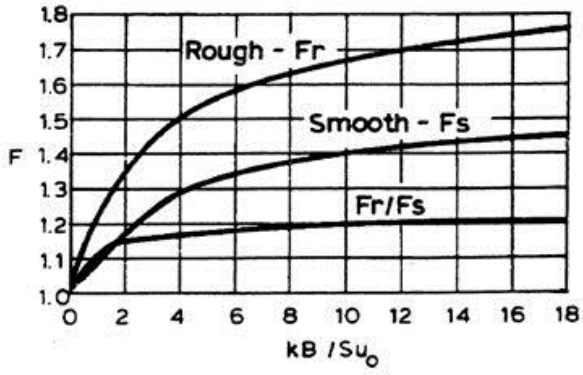

Figure 2.3 – Correction factor, F, from DNV CN 30.4 (1992)

Regarding the bearing capacity factor N_c, many studies have been carried out to determine its value with accuracy. None the less, the solution proposed by Skempton in 1951, shown in Figure 2.4 in function of the foundation and subsoil boundary geometry, is still considered to be adequate.

Correction factors to take into consideration shape (s_{ca}) and depth (d_{ca}) of foundation and load inclination (i_{ca}) are also suggested in DNV CN 30.4 (1992) according to expressions (2) to (4).

Load inclination factor is given by:

$$i_{ca} = 0.5 - 0.5\sqrt{1 - \frac{F_{H1}}{A' s_u}} \tag{2}$$

where F_{H1} represents the horizontal force on the effective area given by the expression: $F_{H1} = F_H - R_{HO} - R_{HP}$, in which F_H is the total force on the foundation, R_{HO} is the sliding resistance

on area outside effective area and R_{HP} is the resistance due to horizontal soil pressure on embedded members.

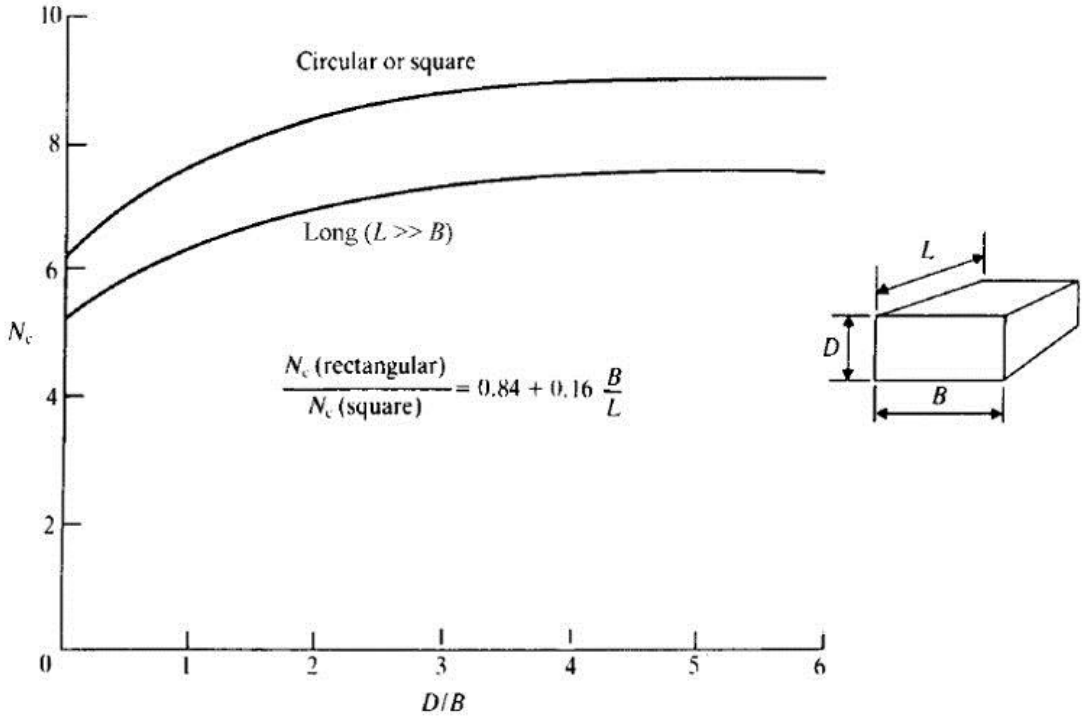

Figure 2.4 – Bearing capacity factor, N_c, in accordance with Skempton, from Atinkson, J. (2007)

Shape factor can be taken as:

$$s_{ca} = s_{cv}(1 - 2i_{ca})\frac{B'}{L} \tag{3}$$

where s_{cv} is given for circular foundations and pure vertical forces as a function of kB'/s_{u_0}, in accordance with Table 2.1.

Table 2.1 – Shape factor given for circular foundations and pure vertical forces, from DNV CN 30.4 (1992)

kB'/s_{u_0}	s_{cv}
0	0.20
2	0.00
4	-0.05
6	-0.07
8	-0.09
10	-0.10

The following expression states the depth factor as:

$$d_{ca} = 0.3\ arctan\frac{D}{B'} \tag{4}$$

Hence all the factors are considered, the resultant bearing capacity is given as the multiplication of the bearing capacity q_u and the effective area *A'*.

$$Q_u = A' \cdot q_u \tag{5}$$

In fact, it is questionable the applicability of classical bearing capacity theories to offshore shallow foundation design under combined loading since it neglects tensile strength that, in reality, can be mobilised by skirts, and there are large components of horizontal load and moment due to the harsh environmental conditions (about 500 per cent greater than onshore). Advanced solution methods, as finite element methods, consider explicitly the three different load components (vertical, horizontal and moment), interacting with each other, for the determination of shallow foundations bearing capacity, through interaction diagrams or failure envelopes (Randolph and Gourvenec, 2011).

2.6.2 Sliding Capacity

Sliding capacity arises as a continuity of bearing capacity. However, as the horizontal failure is independent of foundation geometry and undrained shear strength gradient, it occurs when the applied horizontal force is greater than the soil shear strength at the ground level.

The current rules suggest the calculation of the horizontal capacity as the area multiplied by the shear strength or as a relation between horizontal and vertical force. This relation between vertical and horizontal moments describes a stability envelope as shown in Figure 2.5. The diagram present two curves, correspondent to a null moment or to a moment different from zero. When a case can be represented inside the stability envelope, i.e., behind the curve, the foundation is stable, while the boundary on the right defines the sliding capacity (DNV CN 30.4 (1992)).

$$H = s_u \cdot A \tag{6}$$

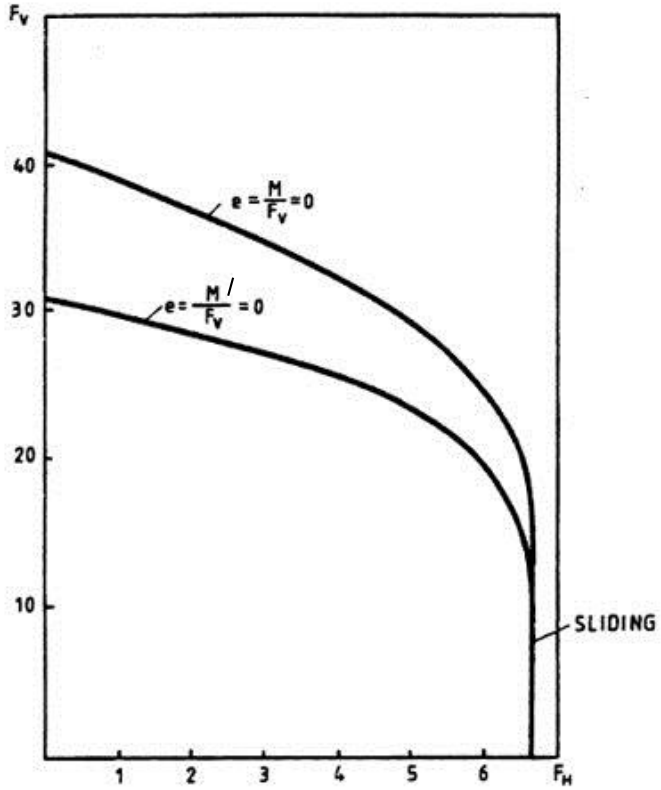

Figure 2.5 – Foundation stability envelope for clay from DNV CN 30.4 (1992)

2.6.3 Safety factor

During design phase, assumptions are made due to several uncertainties. The soil behaviour and the loading are the most critical. Beyond the simplifications made on soil properties and on the load case under consideration, the theoretical equations also have its assumptions. In most cases, both the field conditions and those submitted to the structure during its life are not as simple as predicted by the theoretical equations. This way, it is usual to consider safety factors. The safety can be ensured by different approaches: Working Stress Design (WSD), Load and Resistance Factor Design (LRFD) and probabilistic analyses.

In a WSD approach, a single safety factor is applied to the ultimate limit load. This factor is roughly given as a relation between the resistance and the unfactored applied load, as presented in equation 7.

$$FS = \frac{\sum resistance}{\sum load\ applied} \tag{7}$$

From the safety factor universal standpoint, it is not possible to have an agreement regarding the distinct conditions present at seabed from site to site. Even so, there are general situations

to which normative documents establish safety factors to consider within the design calculations. In terms of offshore shallow foundations the API RP 2A WSD (2005) suggests that the safety factor shall be equal or greater than 2 for bearing capacity and 1.5 for sliding failure, to WSD approaches.

On the other hand, in terms of ULS, the LRFD approach consists on applying partial coefficients to loads and strength, reducing the strength and increasing the loading. ISO 19901-4 (2003) recommends to reduce the shear strength by partial factor of 1.25 and increase the load by 1.1 regarding dead loads or 1.35 for live loads. Throughout the years, this approach have been generally preferred when compared to the WSD. Supporting this the latest revisions of the several standards such as API and ISO, have included this approach. Moreover, Eurocode 7 presents a similar approach applying partial coefficients to loads and strength parameters.

2.6.4 Displacements

Serviceability limit state establishes limits to structures' displacements. In general, allowable settlements are defined by the maximum relative deformation between equipments without compromising the structures' integrity and operation.

In presence of clays, large settlements are expectable since it is a very compressible soil, with high voids ratio, even more when saturated. As known, clayey soils show extremely low permeability, which when loaded causes accumulation of pore pressure at a short term. Along the time, the excess pore pressure dissipates, the consolidation process occurs and large settlements happen.

Settlement control is an important issue in structures' design since it can be more restrictive than bearing capacity concerns. In order to plan the operations required to connect the pipeline to the equipments only when most settlement has occurred, it is also important to predict its magnitude and the time until it occurs.

Frequently, the long term settlement is the most critical concern, but once there are heavy loads applied by the equipment, the short term settlement may also be a concern since it can affect the normal operation of the equipment or even damage and disable it.

Other displacements such as horizontal movements and rotations, in general, only occur immediately with load application (Randolph and Gourvenec, 2011).

Short Term Displacements

This is the settlement that occurs immediately after the structure is landed, in undrained conditions, and is usually due to elastic distortion of the soil. This settlement is not elastic because the soil has a nonlinear behaviour. However, most theories are based on the elasticity theory and are applicable to homogeneous, isotropic and linear elastic materials.

At a short term there are horizontal and vertical displacements as well as rotations, but the vertical settlements are the most significant. For this reason those are the main displacements analysed.

The settlement can be calculated in function of the Young's Modulus and the Poisson's ratio, the mudmat dimensions and the applied loading, as presented in equation (8), deducted from Boussinesq's theory for a rigid circular foundation with diameter B. To computing applications other methods derived from the referred theory are widely used since they provide accurate results.

$$u_v = \frac{\pi}{4} qB \frac{(1-\nu^2)}{E} \tag{8}$$

where q is the uniformly distributed load.

As the settlement is experienced in a short time, there will not be enough time for soil mass for change in its water content. Hence, settlement takes place under constant volume or under undrained conditions. Therefore the magnitude of the settlement highly depends on the shear strain and effective stress.

In cohesive soils that may suffer large settlements, besides the theoretical expressions, numerical analyses are recommended as a more accurate approach to predict the settlements.

To estimate the immediate horizontal displacement, it is recommended the following expression (API RP 2A WSD, 2005):

$$u_h = \left(\frac{7-8\nu}{32(1-\nu)GR}\right) H \tag{9}$$

Long Term Settlements

The process of consolidation starts when excess pore pressure dissipation takes place and depends on permeability, compressibility and thickness of the soil layers. This process can be described as the transition of the load from the pore fluid to the soil skeleton.

In grained soils, that have high permeability, settlement only occur at a short term, once the pore pressure dissipation is virtually instantaneous. On the other hand, fine soils, as clays, have very low permeability which makes them very affected by the long term consolidation.

In contrast to immediate settlements, that happen in undrained conditions, during consolidation the volume change is noticeable. It includes mainly two stages: primary and secondary consolidation. This phase can be distinguished by the time rate and the type of compression they are due. During the water expulsion from the voids, the excess pore water dissipates and the stress is progressively transferred to the soil skeleton. This process is called primary consolidation. Secondary consolidation is caused by creep, i.e. the increase of deformation occurs at constant stress level (the excess pore water have already dissipated).

For normally consolidated soils (OCR ≤ 1), which are the typical soils at deep water depths, settlements due to primary consolidation can be predicted using the following expression:

$$u_{v,pc} = \frac{H_0}{1 + e_0} C_c \log\left(\frac{\sigma'_{vf}}{\sigma'_p}\right) \tag{10}$$

There is not an exact moment that defines the end of primary consolidation and the beginning of the secondary. It is common to assume that primary consolidation ends when 95% of settlements have occurred. Using the average degree of consolidation, *U*, and consulting specific tables, it is possible to obtain the time factor, T, used to calculate the average time that primary consolidation will take.

$$T = \frac{c_v t}{d^2} \tag{11}$$

Hence, to predict settlements occurred over a given period after the end of primary consolidation, secondary settlements, is used the following expression:

$$u_{v,sc} = \frac{H_0}{1 + e_1} C_\alpha \log\left(\frac{t_2}{t_1}\right) \tag{12}$$

2.7 Constitutive Soil Model: Mohr-Coulomb

As seen previously, the foundation stability is ensured by taking into account the soil strength profile, which, in addition to the shear strength parameters, depends on the stress and strain levels and stress path.

Since the beginning of the studies about soil behaviour, several strength criteria have been proposed, the Mohr-Coulomb being one of the simplest and more often used. This model is a

linear elastic perfectly plastic model, which is based on Hooke's law (linear elastic part) and on Mohr-Coulomb failure criterion (perfectly plastic part). Over the years, this model has become the most popular as a result of its reasonable adjustment to reality combined with the small number of parameters required.

Elastoplasticity basic principle determines that strains can be decomposed into two parts, as shows Figure 2.6: elastic and plastic.

$$\varepsilon = \varepsilon^e + \varepsilon^p \tag{13}$$

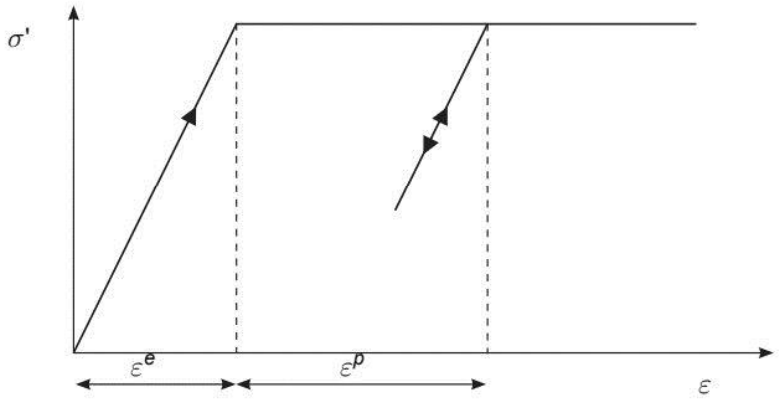

Figure 2.6 – Basic principle of elastic perfectly plastic model (Plaxis, 2015)

To evaluate if plasticity occurs in a calculation, it can be analysed the yield surface, shown in Figure 2.7, which is defined by model parameters and not affected by plastic strains. This surface can be understood as the surface that divides the purely elastic behaviour of the soil, inside the surface, from the plastic behaviour related with irreversible strains (Plaxis, 2015).

This linear elastic perfectly plastic model requires elastic parameters: Young's modulus and Poisson's ratio ν, and plastic parameters cohesion c, friction angle ϕ, dilatancy angle ψ and tensile strength σ_t.

The use of the model and its parameters in the software will be described later in this report.

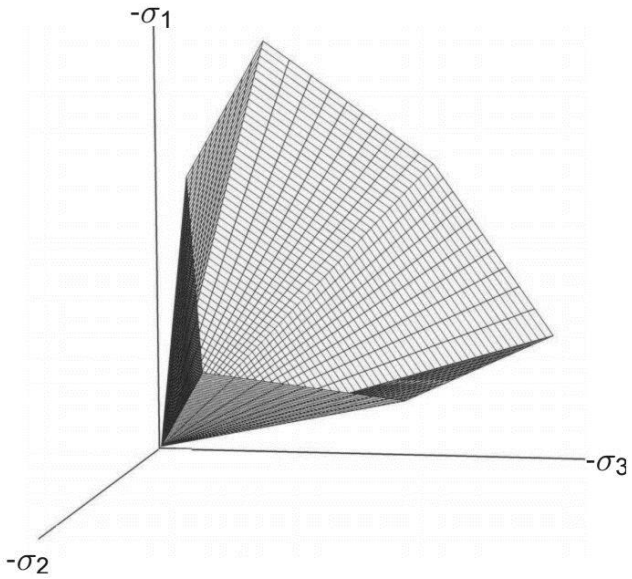

Figure 2.7 – Mohr-Coulomb three-dimensional yield surface in principal stress space (Plaxis, 2015)

3 FINITE ELEMENT MODEL

3.1 Introduction

The assessment of soil behaviour loaded by mudmat foundations requires the analysis of the stresses, strains and settlements, which will vary in function of the applied loading. For that reason and in order to analyse what happens immediately after the installation, the study was conducted using three dimensional finite element analyses, using a recent software from Rocscience, *RS3*.

In order to define a reference to all the future analyses, presented in the next chapters, it was defined a base case model. Some parameters were tested and their influence were evaluated. Finally, the model was validated according to the Theory of Soil Mechanics. This case is kept throughout the different models present along the next chapters.

In the present chapter the modelling approach used for the base case is detailed, as well as the validation of the model and the respective results. The organization of the present chapter follows the input data sequence in RS3.

3.2 Numerical Modelling

3.2.1 Geometry and support

The base case considers a 5x10 m^2 rectangular solid mudmat without perforations. The external dimensions of the model were defined in order to reduce as much as possible any influence on the stresses distribution. Thus, it was defined a 25 x 35 x 15 m^3 (B x L x H) volume which gives sufficient margin beyond the mudmat extremes, as represented on Figure 3.1.

It should be referred that, as long as no load eccentricity is considered, the problem is symmetric in two directions and a quarter of the whole model could be used in the analysis. However, as on subsequent analyses non symmetrical loading was applied, the whole model was used in all calculations to maintain consistency.

The mudmat geometry was defined according to the usual geometries adopted for subsea structures, i.e., rectangular with a ratio *B/L* of about 0,5. Hence, the modelled foundation has

an area of 50 square meters and is modelled as a steel plate with elastic properties, shown in Table 3.1. Its stiffeners are not physically modelled, but their effect is considered by an equivalent thickness, as if they were 30 cm in length.

Table 3.1 – Mudmat properties

Dimensions (m²)	5 × 10
Thickness (m)	0.10
E (GPa)	210
ν	0.3
Material Type	Elastic

As shown in Figure 3.2, the software allows to specify the support behaviour as elastic or plastic. In this case the elastic was chosen as the stress level on the mudmat does not constrain the safety neither the settlements. It is also important to note that checkbox "*Include Weight in Analysis*" is not checked since the mudmat self-weight is included in the analyses by the applied loading.

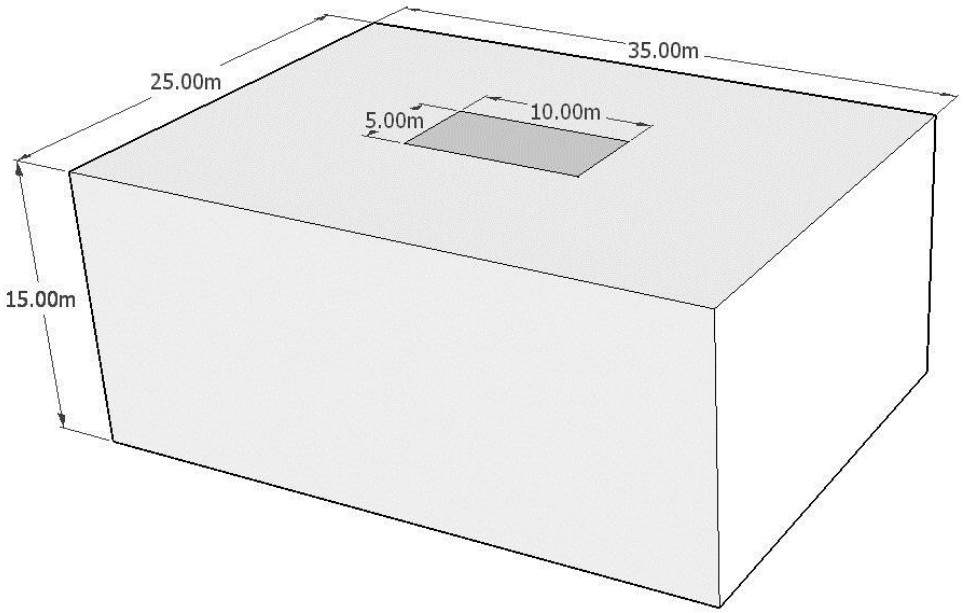

Figure 3.1 - Model geometry

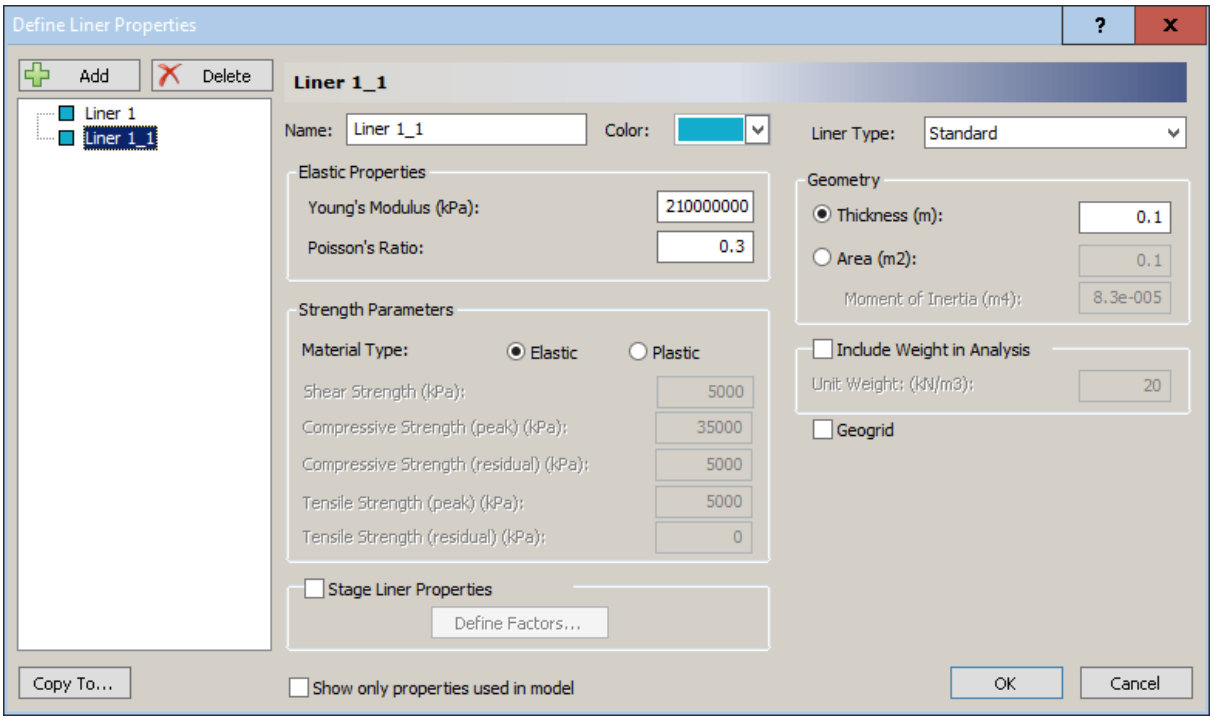

Figure 3.2 – Input of support properties

3.2.2 Soil Properties

The analyses are based on soil samples from West Africa, more precisely on Angola's coast. The geotechnical parameters for the foundation design were derived from the results obtained after the soil characterization through *in situ* and laboratory tests. Those tests have shown a normally consolidated very soft clay of high plasticity.

As seen previously, for cohesive soils, clayed soils, which are normally consolidated the most critical phase in terms of stability and settlements is the short term, after the load is applied. At this phase, the soil has an undrained behaviour, due to its low permeability, which, in terms of shear strength, is characterised by a null friction angle ϕ and the undrained shear strength, s_u. Using these parameters, undrained total stress analyses were performed.

Bearing this in mind, the soil was modelled as a linearly elastic perfectly plastic material, governed by Mohr-Coulomb failure criterion.

Before yielding, during elastic behaviour, the soil properties can be defined, in the input window showed in Figure 3.8, as *isotropic*, *transversely isotropic*, *orthotropic* or *hyperbolic*. It was considered that the soil has the same properties in all directions, i.e., it's isotropic. Thereby, stiffness is modelled considering the undrained Poisson's ratio and the undrained Young's

Modulus in addition to strength parameters, the friction angle set to 0º and the cohesion c set to s_u.

For undrained conditions, the Poisson's ratio assumes values close to 0.5. Once this value can lead to singularities of the stiffness matrix, a value of 0.495 was chosen.

The deformability is controlled by the Young's Modulus but also by the Poisson's ratio. This parameter usually show an *in situ* increase with depth. On a first approach, it was used a linear relationship in depth, with exception to the two first meters where this parameter presents a small peak possibly due to sedimentation and chemical reactions (strongly cemented thin layer). Due to the low values available for Young's Modulus in this soil, it was considered the expression proposed by Duncan and Buchignani (1976), which relates the Young's Modulus with the undrained shear strength (Matos Fernandes, 2011). The expression considered is:

$$E_u = 600 \times s_u \tag{14}$$

Although RS3 allows the use of datum dependent modulus, increasing linearly with depth, to better represent the real soil behaviour, some inconsistencies were noticed during calculations, when this property was used. For that reason, the soil was divided by layers each one with a constant value of Young's Modulus fitted to the second linear approach.

Figure 3.3 presents the profiles described above.

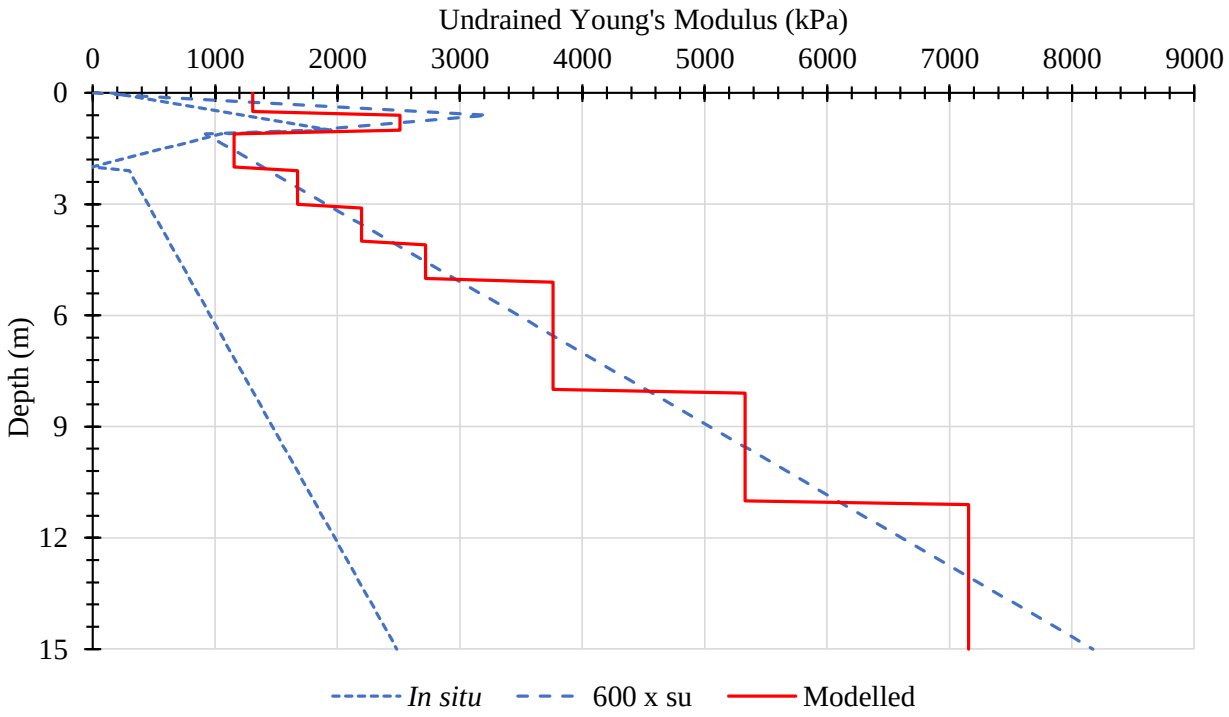

Figure 3.3 – Undrained Young's Modulus profiles

Similarly to the Young's Modulus, the undrained shear strength also shows a linear increase with depth and a peak on its values, as seen in Figure 3.4. Moreover, each material layer was defined with a constant value of s_u, even though, in this case, no inaccuracies were found on the results, when datum dependent s_u was used.

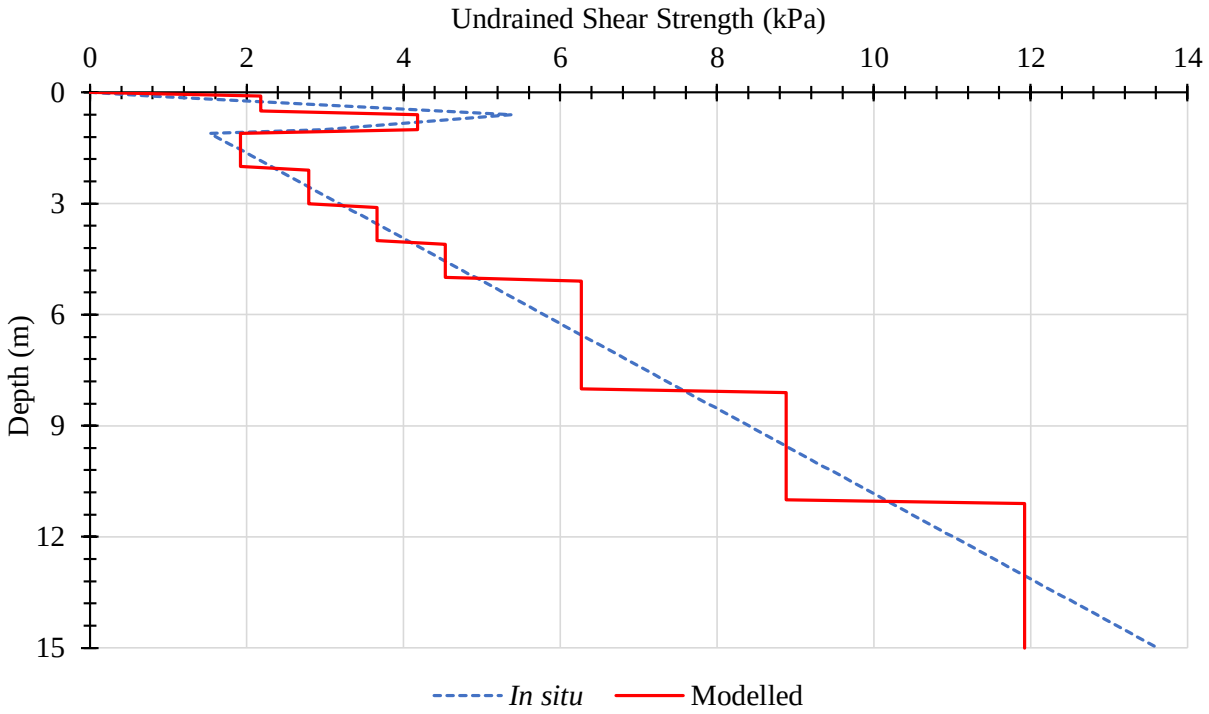

Figure 3.4 – Undrained Shear Strength Profile

At surface level, where the stress level is low, tensile stresses are expected, mainly around the mudmat and inside its holes. These tensile stresses are due to the zero volumetric strains associated to the undrained soil behaviour. Although it is well known that the soil does not present tensile strength, when analyses were performed using the tensile strength set as 0 or with a low value, due to the low stress values at surface, the failure occurs in those areas, contrarily to reality and to the analyses purpose. Consequently, to avoid the issue highlighted previously it was used a high value for the tensile strength. However, the use of a high value for tensile strength in clays is questionable.

Therefore, in order to ensure that the high value has a small influence in the results, plane strain analyses were performed. These analyses were carried out using a 2D finite element software, RS2. The model represents the mid-section of the 3D model (in RS3) in Y direction, as shown in Figure 3.5. Both material and support properties were the same as the 3D model described in this chapter. Figure 3.6 presents the vertical stress and the deformed mesh.

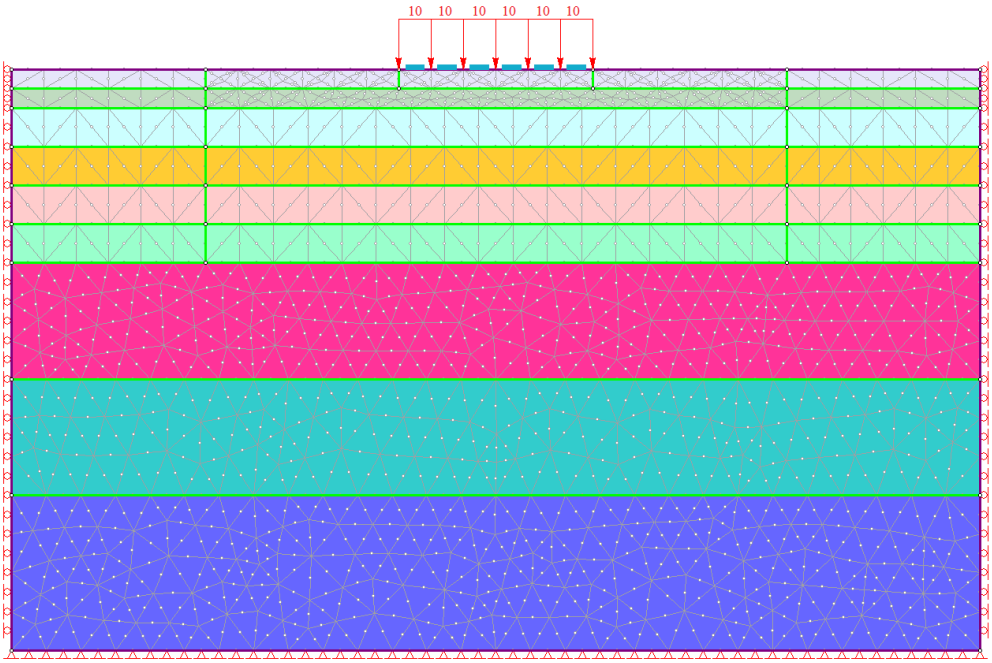

Figure 3.5 – 2D Model

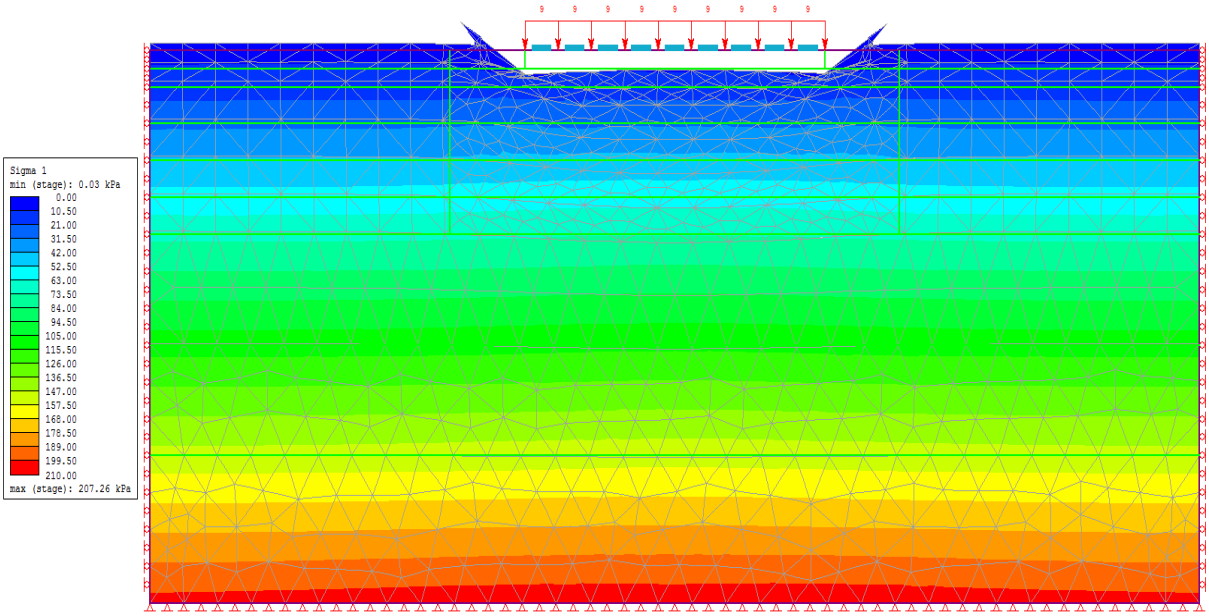

Figure 3.6 – Vertical stress and deformed mesh of the 2D model

The analyses showed a maximum of 0.2 kPa of tensile stress when it was not applied tensile strength ($\sigma_t = 0$ kPa) and 2.72 kPa when it was used 10 kPa or 10^7 kPa of tensile strength. As shown in Figure 3.7, impact of the tensile strength in displacements is almost null. Thus, the use of a high value for tensile strength has a negligible effect.

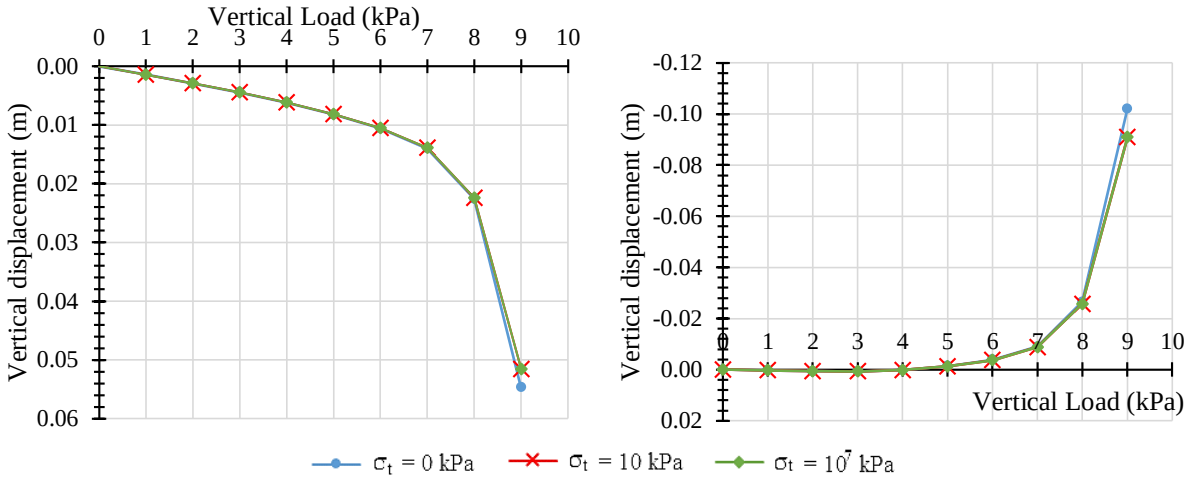

Figure 3.7 – Vertical displacements in 2D model: a) bellow the centre of mudmat and b) 0.5 m distant from the mudmat side

Regarding the initial element loading, i.e., the loading before the application of external forces, RS3 allows to consider *Field Stress Only*, *Field Stress & Body Force*, *Body Force Only* or *None*. The *Field Stress & Body Force* option was adopted, which considers not only the soil weight but also the stress level at each depth. The unit weight was stablished as the saturated unit weight since it is at the bottom of the ocean.

As the soil stress state reaches the yield surface, its behaviour becomes plastic and assumes its plastic properties. In this case, it was considered the same values for elastic and plastic strength parameters (tensile strength, undrained shear strength and friction angle).

Table 3.2 summarizes the soil properties used to define the soil in RS3, taking all the above into account and the input window for material properties in RS3, shown in Figure 3.8.

Table 3.2 – Resume of soil properties

	Layer Depth (m)	***ν***	***E_u (kPa)***	***s_u (kPa)***	***γ (kN/m³)***	***Failure Criterion***	***Tensile Strength (kPa)***	***Material Type***
Material 1	0-0.5		462	0.8	13			
Material 2	0.5-1.0		3228	5.4	13			
Material 3	1.0-2.0		918	1.5	13.5			
Material 4	2.0-3.0		1184	2.0	13.5			
Material 5	3.0-4.0	0.495	1705	2.8	13.5	Mohr Coulomb	10^7	Plastic
Material 6	4.0-5.0		2227	3.7	13.5			
Material 7	5.0-8.0		3531	5.9	13.5			
Material 8	8.0-11.0		5095	8.5	13.5			
Material 9	11.0-15.0		6921	11.5	13.5			

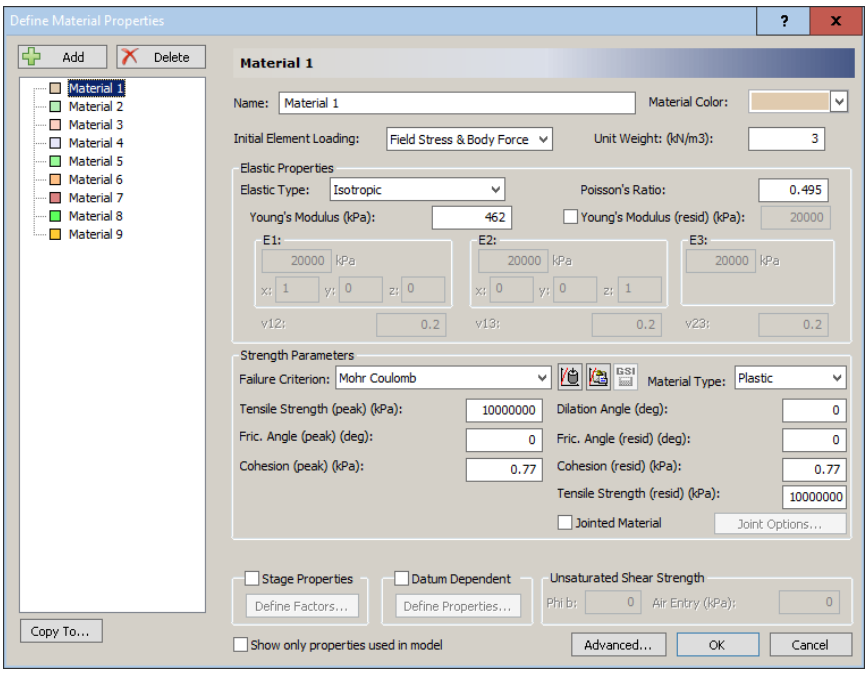

Figure 3.8 - Input of material properties

3.2.3 Loads and Restraints

After the geometry and materials are defined, the boundary conditions of the model and the applied loads were added.

Since the applied loading has no influence in the boundaries, the displacements were restrained in the perpendicular direction of each surface on external boundary and in both X and Y directions in each vertical edge, as shows Figure 3.9. At bottom, all displacements are restrained.

During the study, several analyses were carried out and the loading was adapted at each objective. In a first step, it was only considered a purely vertical loading, with magnitude increasing at each stage. For the base case the first loading approach is showed in Table 3.3. The load was applied as a uniform loading, in order to ensure that the stresses transmitted to soil were uniform under the mudmat. In models with perforation, the values of the uniform loading were maintained and the total load varies in function of each mudmat area. The loading was applied according to the sign convention shown in Figure 3.9. The measured results presented throughout this document follow also the same convention.

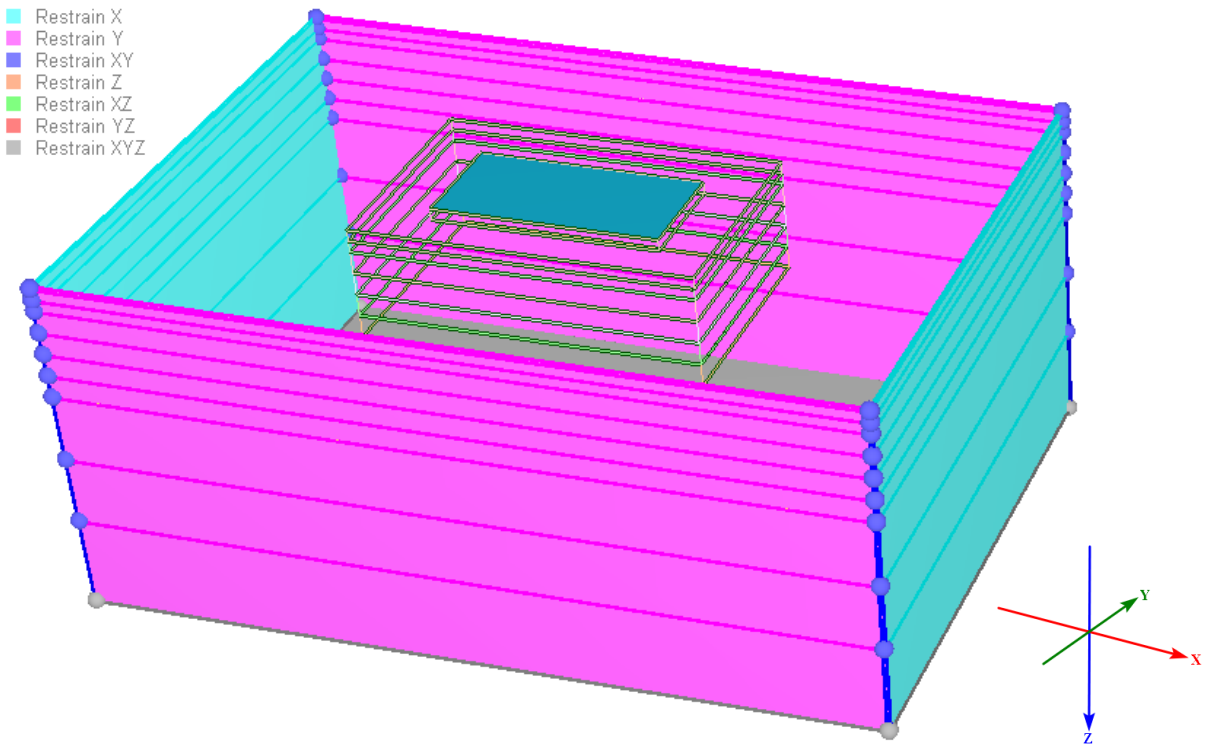

Figure 3.9 – Model restraints

Table 3.3 – Vertical Load to Base Case model

Stage	***1***	***2***	***3***	***4***	***5***	***6***	***7***	***8***	***9***	***10***	***11***	***12***	***13***	***14***	***15***	***16***
Total Load (kN)	0	500	600	700	750	800	820	840	860	880	900	920	940	960	980	1000
Uniform Load (kN/m^2)	0	10	12	14	15	16	16.4	16.8	17.2	17.6	18	18.4	18.8	19.2	19.6	20

3.2.4 Mesh

The last phase of the input in RS3 is the mesh generation.

The soil was defined using 10-node tetrahedral elements in a graded distribution, with 4 integration points (Gauss points). This type of elements corresponds to quadratic elements (second order of three dimensional finite elements), developed from the linear tetrahedral elements of 4-nodes, by adding 6 additional nodes at the middle of each edge, as shown in Figure 3.10. The element deformation can be derived, in function of the stress level and its

shape functions (determined at each element's node). The stress is determined in the Gauss points and then extrapolated to the external nodes.

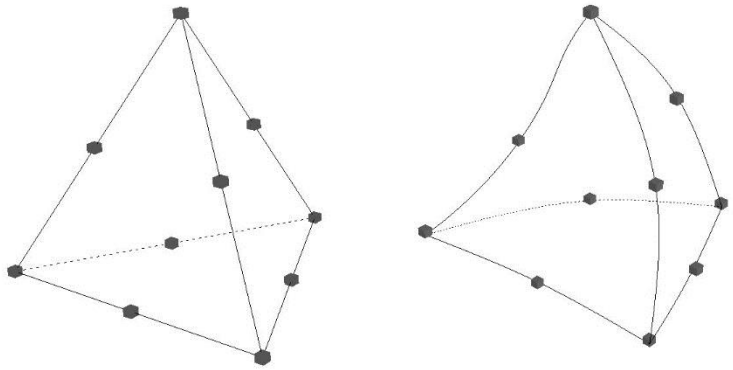

a) b)

Figure 3.10 – 10-node tetrahedral finite element: a) undeformed and b) deformed shapes

Regarding the mudmat, 6-node triangular shell finite elements were used. This type of element is derived from the 3-node triangular shell elements by adding 3 nodes on each mid-side and corresponds to the second order of two dimensional finite elements, i.e., quadratic elements.

In the contact between the two types of elements (shell and three-dimensional finite elements), the displacements are in accordance with the freedom degrees of each element. The shell elements allow 3 translations and 2 rotations at each node while the tetrahedral elements only allow 3 translations at each node and no rotations.

The software allows to control the mesh density in two ways: by controlling the density of elements in all the model, increasing or decreasing the *Number of Edges on External Boundary*, and by applying a multiplier factor in selected volumes, surfaces or edges, as shows the input windows in Figure 3.11. For the present study the first method was set constant in all models and the second method was used to control the number of elements and nodes. RS3 also enables to see the mesh quality and to control the parameters of quality.

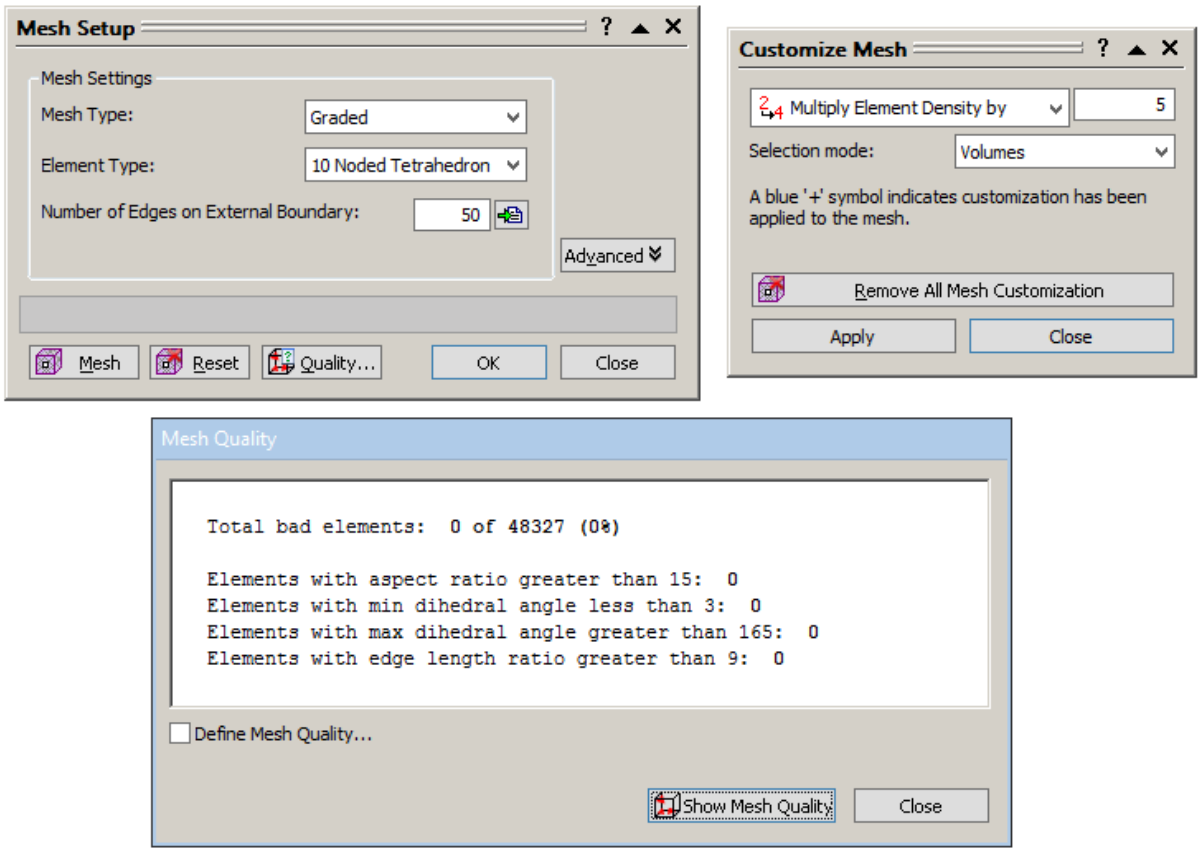

Figure 3.11 – Inputs of mesh setup, customization and quality

It is well known that the finite element mesh has a large influence on the results, as it stablishes the number of points where the displacements and stresses will be calculated, determining the accuracy of the analysis.

In order to obtain accurate results, the number of elements and nodes was studied and adjusted based on the depth of refinement and the multiplier factor. First of all, four different depths were stablished to be refined – down to 0.5 m, 1 m, 3 m and 5m. For each of these depths, three multiplier factors were used – 3, 5 and 10. The applied load, showed in Table 3.4, differs from the applied on the base case approach.

Table 3.4 – Applied uniform load to analyse mesh influence

Stage Number	*Uniform Load (kN/m²)*
1	0
2	10
3	12
4	14
5	16
6	18
7	20

Observing Figure 3.12, it is possible to conclude that, independently of the depth refined, as the multiplication factor increases, and hence the number of elements, also the results converge to the same value of displacement. Regarding the stage in which all the analyses shown good results (10 kPa), the three curves present almost the same settlement. For that reason, a multiplication factor of 5 was used in the several analyses in this document (with a few exceptions as explained in the text below).

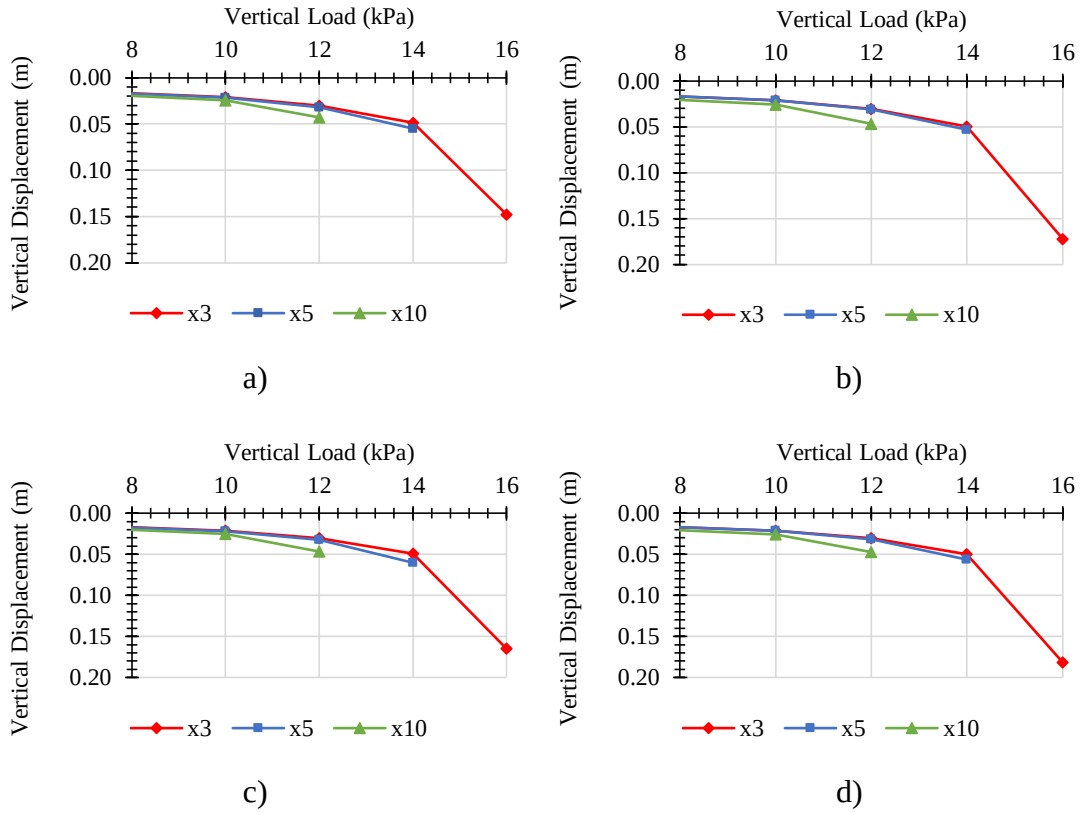

Figure 3.12 – Vertical displacements when refinement is: a) up to 0.5 m; b) up to 1m; c) up to 3 m and d) up to 5 m

Analysing the same displacements in contrast with the depth of refinement with the same multiplier factors, it is noted that, based on Figure 3.13, the depth of refinement has a small impact for the measured displacements, in this case.

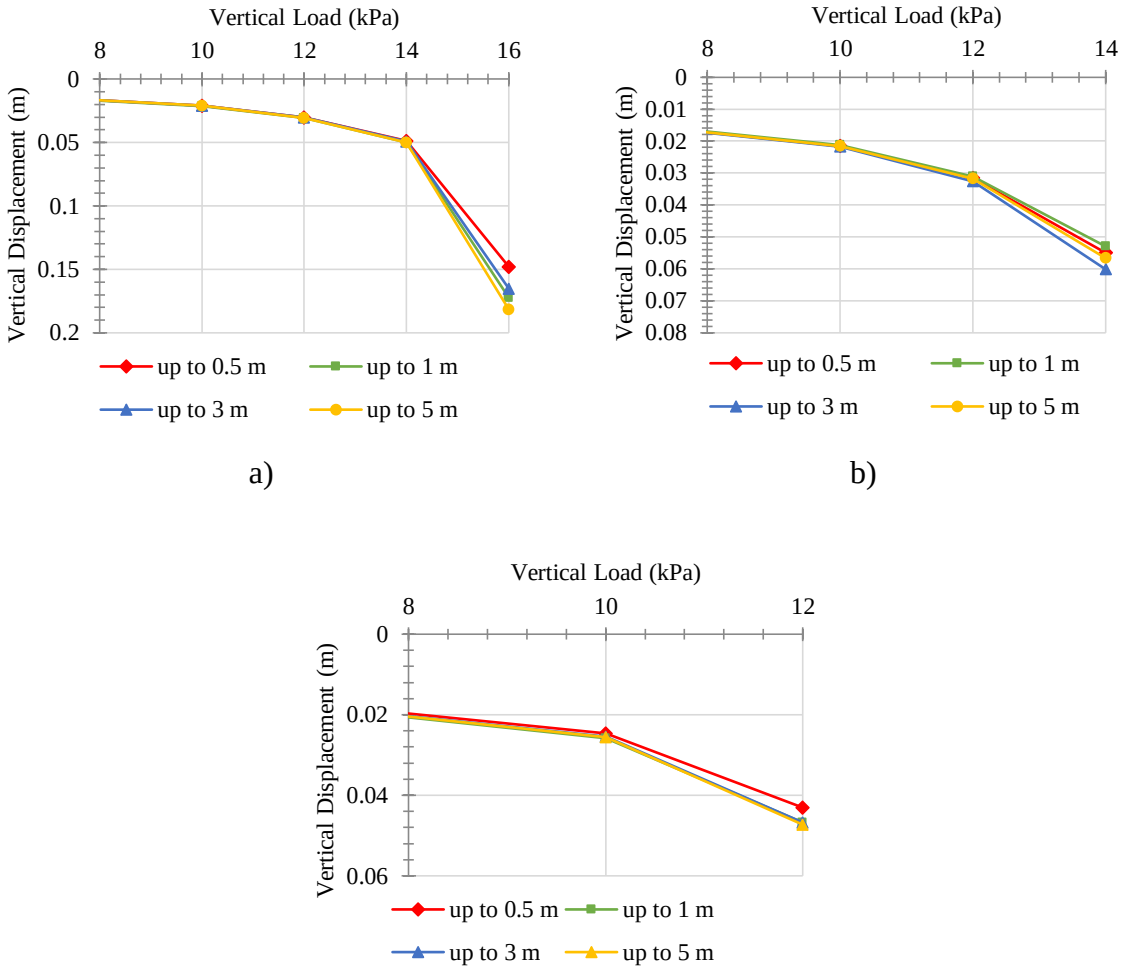

Figure 3.13 – Vertical displacements when refinement is obtained using a multiplier factor of: a) 3; b) 5 and c) 10

On the basis of the above, the mesh was generated using 50 edges on external boundary and a multiplier factor of 5 down to a depth of 1 meter below the mudmat, as shown in Figure 3.14.

Even though this solution leads to good results on the model described above, during calculations some irregularities were noticed. Especially, in models which the mesh has more than 100 000 nodes in the whole model. These models are characterised for having many points at the surface, which leads to a very refined mesh. The software creates mainly vertical thin elements in those areas, leading to numerical errors when the results are extrapolated from the Gauss points to the elements nodes.

In conclusion, the mesh was generated independently in each model, taking into account the above conclusions but also the number of nodes and the elements shape.

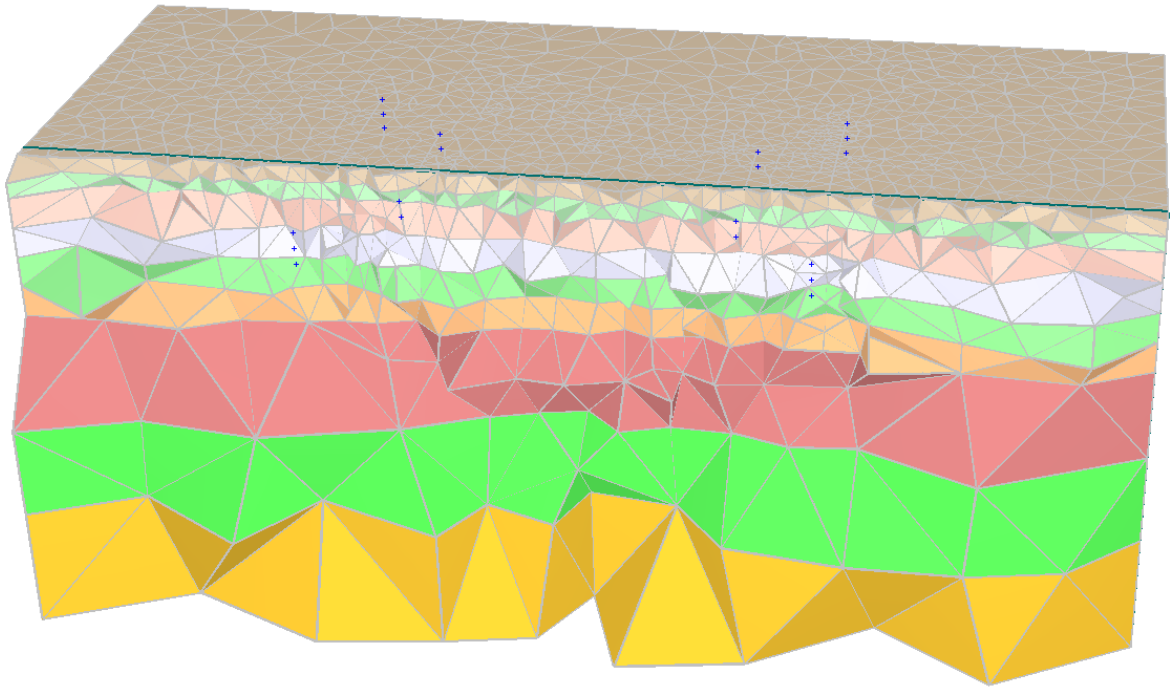

Figure 3.14 – Finite elements mesh for the base case: 68224 nodes and 48327 elements

3.3 Validation

When analysing the results given by a software for any model, it is important, firstly, to evaluate their reliability and agreement with the theory and, secondly, to verify if the initial conditions of the model, i.e., the stresses, displacements and other relevant information, are as expected for the case under study.

With this purpose, and since some restrictions were noticed on the software when using some properties varying with depth by applying an increase factor, the software was tested by the simulation of triaxial tests with elasto-plastic analyses. These tests were modelled as shown in Figure 3.15 and the vertical stress was increased until failure. The different properties (undrained shear strength, friction angle and Young's Modulus) were set increasing with depth in turns. The results were then compared with soil mechanics, proving its reliability as seen in Figure 3.16. Except when it is used specific parameters varying with depth, such as the friction angle and the Young's Modulus.

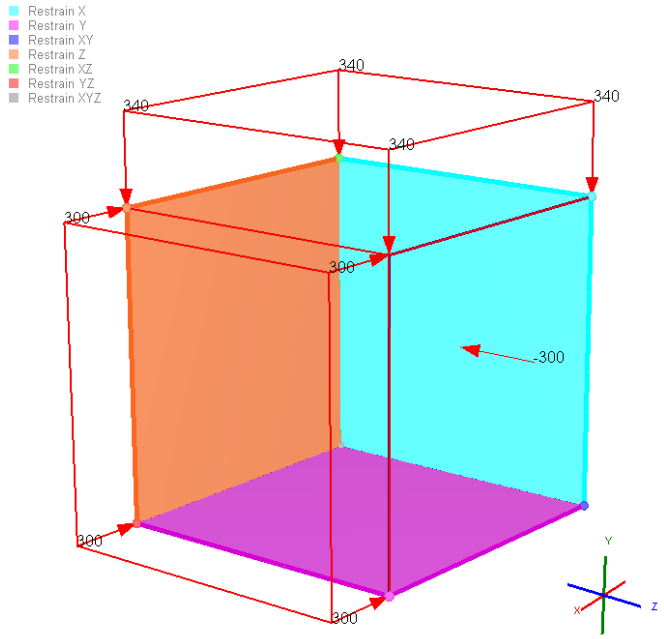

Figure 3.15 – Triaxial test model

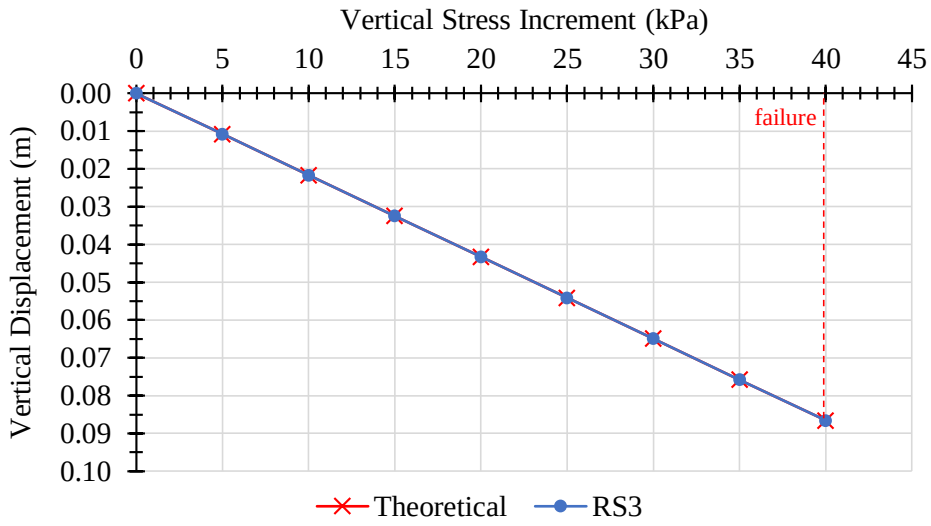

Figure 3.16 - Results comparison between theoretical and RS3 displacements, for a triaxial test, without properties varying with depth

Concerning on the base model used for this dissertation and, as explained before in this document, all the input data was entered considering the software limitations, preventing possible inaccuracies.

Regarding the initial conditions, the stress in vertical direction, shown in Figure 3.17, presented the expected profile and the vertical displacements are null, or very close to zero due to the

body force, considering that there's no external forces applied. The settlement in the stage before failure is shown in Figure 3.18.

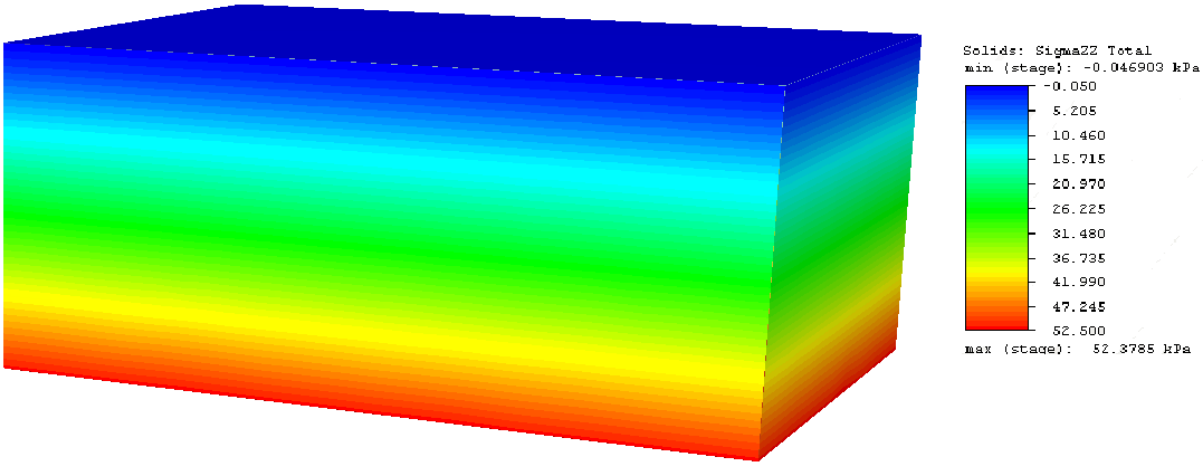

Figure 3.17 – Initial Stress in vertical direction

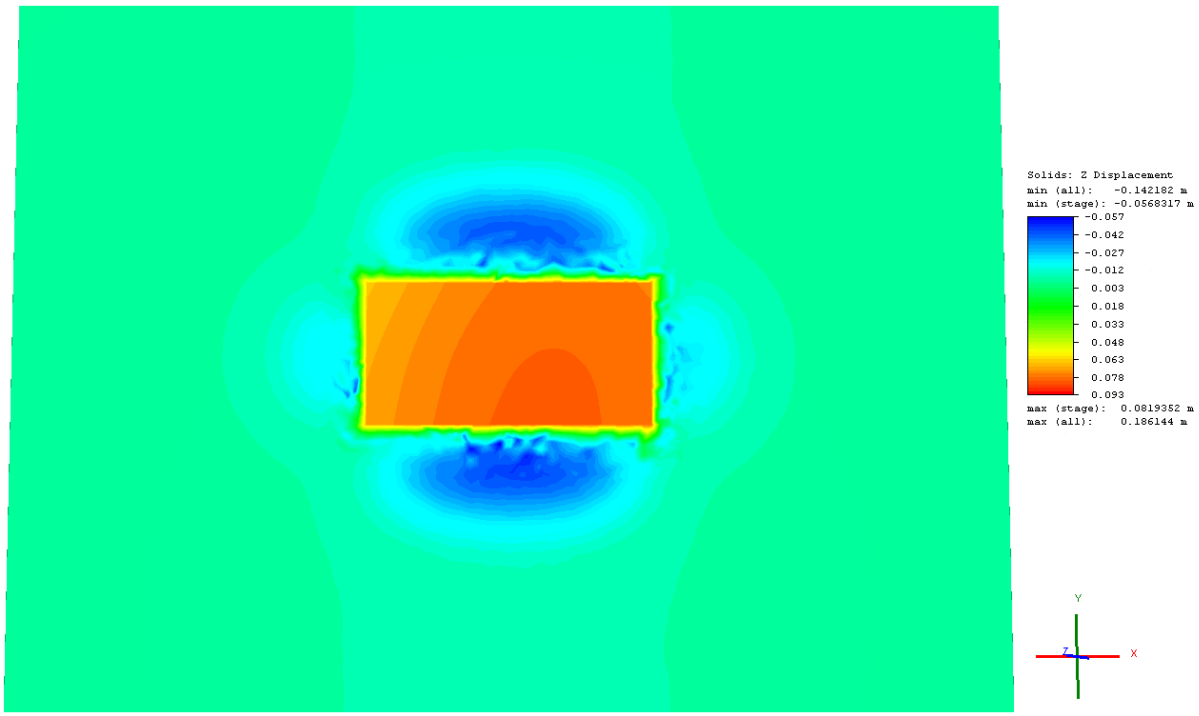

a)

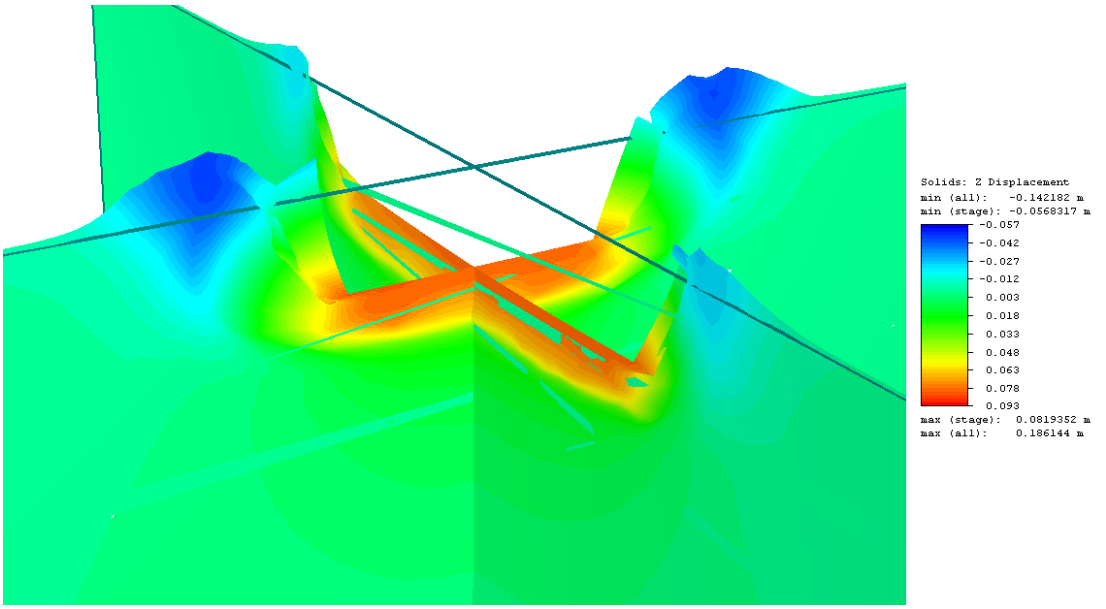

b)

Figure 3.18 – Base case settlements before failure: a) top view and b) cross sections

4 RESULTS AND DISCUSSION

4.1 Introduction

This chapter aims to detail and discuss the influence of perforations in a mudmat bearing capacity. The analysis focuses on two main points: the influence of holes' arrangement; and the effect of the perforation ratio. However, the variation on holes' shape and the behaviour of a perforated mudmat under combined loads are also analysed.

The models kept the same geometry, soil properties and support properties as the base model varying only the number of holes, their diameter and arrangement.

To be able to do a proper analysis and comparison of all the models, at the beginning it was set the reference of comparison defining what to be measured and also where it would be measured. There are several methods to analyse a foundation bearing capacity: analyse its ultimate load; determine its safety factor; analyse its load *vs* displacement curve. Within this document, the vertical displacements are the main data type analysed to evaluate the influence of the different parameters, by comparing the several models with the base case described above, i.e. a solid mudmat.

Regarding the reference point, it was important to analyse a point that would exist in the several models to be able to compare their results. Moreover, this point should also represent the behaviour of the foundation. The central point was the data point chosen until the perforation arrangement did not match with it. Once the mudmat central point wasn't part of the support a second point, the middle point of one of the mudmat boundaries, was considered.

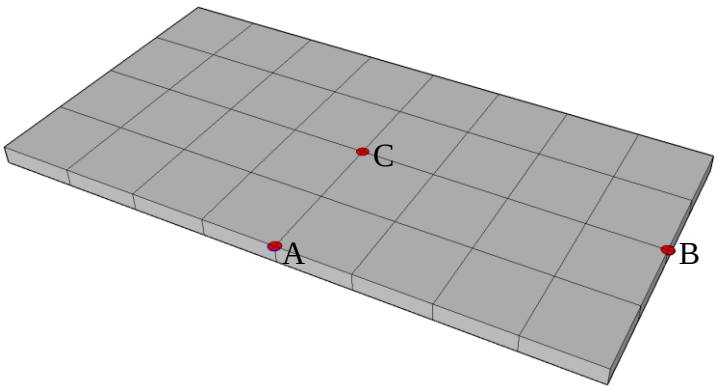

Figure 4.1 – Possible reference points to measure the results

In order to select which boundary better represents the mudmat displacements, the vertical displacements of each one in function of the loading were analysed. As can be seen in Figure 4.2, the boundary in *X* direction presents higher vertical displacements values. For this reason, in following subchapters, the results presented are based on this point (point A, except when mentioned).

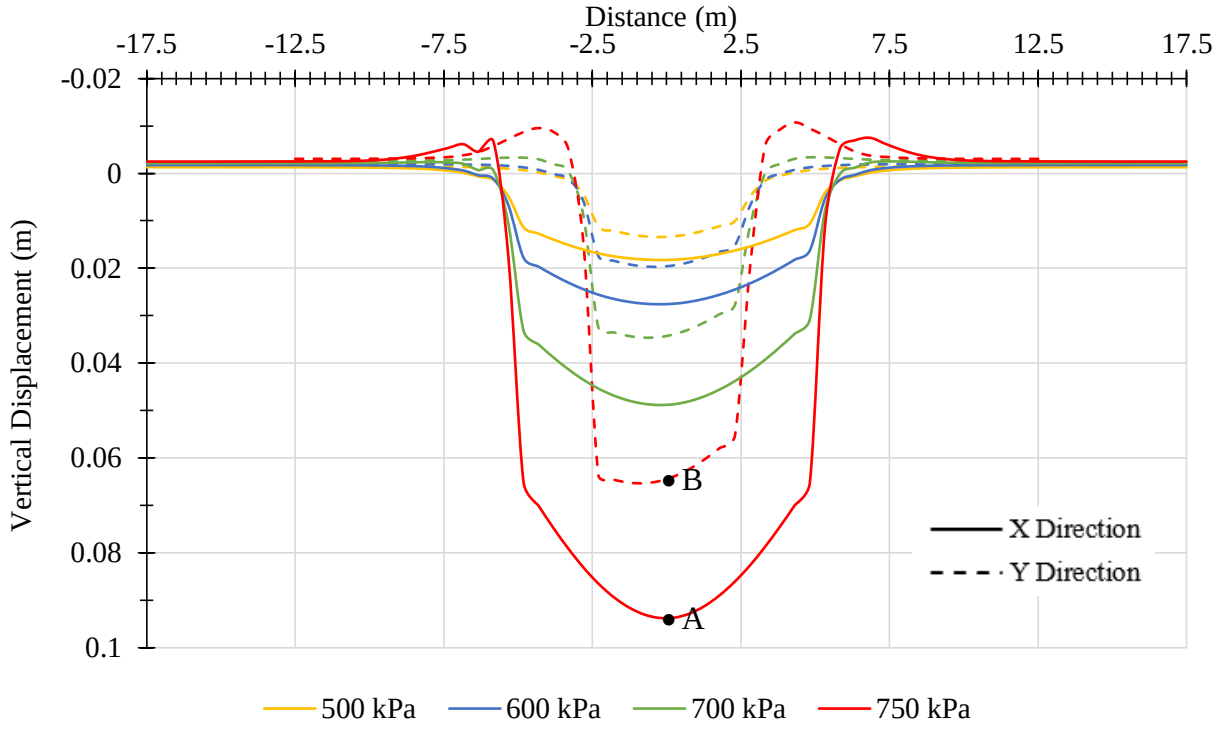

Figure 4.2 - Vertical displacements in mudmat boundaries

The nomenclature used for the RS3 files is based on the number of holes, holes diameter and perforation ration as presented below.

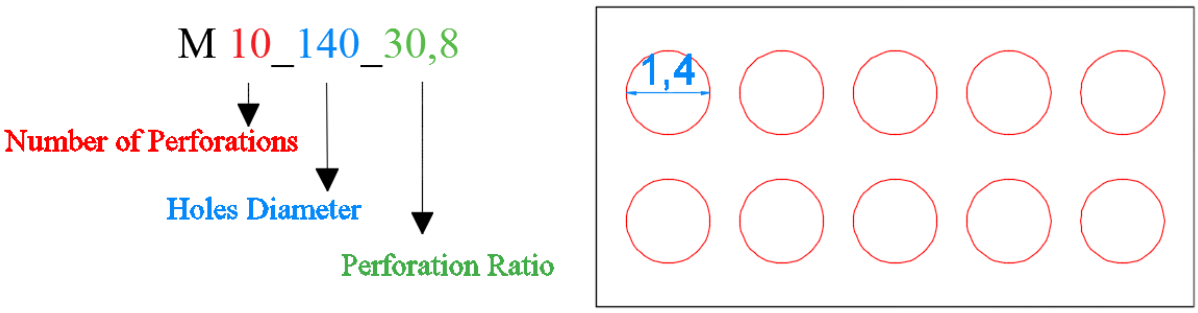

Figure 4.3 – Nomenclature exemplification

The short form *M 10_140_30,8* refers to a model with 10 holes, each one with 140 cm of diameter and a perforation ratio of 30,8%. In cases that the holes have different diameters it referred using a "+", as for example *M 13_120+200_33,4.*

4.2 Influence of Holes' Arrangement

From the standpoint of the installation process, it is expectable that a solution with wider holes corresponds to a better solution, once it reduces significantly the installation forces, preventing the structure to suffer serious damages, and relieving the crane capacity. On the other hand, wider holes increase the displacements and reduce the mudmat bearing capacity. Therefore, it is important to study a balance of these two processes in order to find an optimal solution.

As concluded by White et. al. (2005) the optimal mudmat design comprises a large number of perforations. Thus, it was needed to understand the effect of the number of holes and its arrangement in a mudmat bearing capacity. And also to strengthen his conclusion through numerical analyses.

Regarding the structure bearing capacity, ten different holes configurations, as shown in Figure 4.4, with close perforation ratios were studied in a first approach.

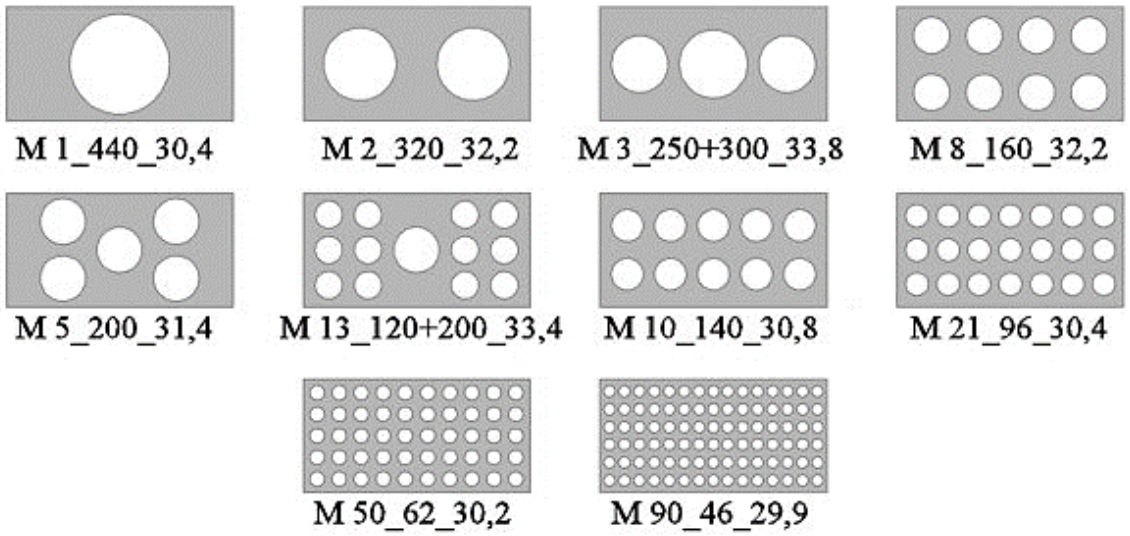

Figure 4.4 – Different holes' arrangements

Each model was designed with a different number of perforations and different diameters. Thus, Table 4.1 presents a description of each model analysed during the first approach.

Table 4.1 – First models description

Model	*Nº of Holes*	*Holes Diameter (m)*	*Perforated Area (m^2)*	*Perforation Ratio*
M 1_440_30,4	1	4.40	15.21	0.304
M 2_320_32,2	2	3.20	16.08	0.322
M 3_250+300_33,8	3	2.50+3.00	16.89	0.338
M 8_160_32,2	8	1.60	16.09	0.322
M 5_200_31,4	5	2.00	15.71	0.314
M 13_120+200_33,4	13	1.20+2.00	16.71	0.334
M 10_140_30,8	10	1.40	15.39	0.308
M 21_96_30,4	21	0.96	15.20	0.304
M 50_62_30,2	50	0.62	15.10	0.302
M 90_46_29,9	90	0.46	14.96	0.299

Analysing the load *vs* vertical displacement (measured in point A) curves, presented in Figure 4.5, it can be observed that, during the foundation elastic behaviour, the perforations have, in general, a small impact in the displacements. However, as the load increases and the foundation gets in the plastic behaviour there are disparities towards the base case model. When observing the curves it is noticed that, as concluded by White et. al. (2005), by increasing the number of holes the curves tend to become closer to the base case behaviour.

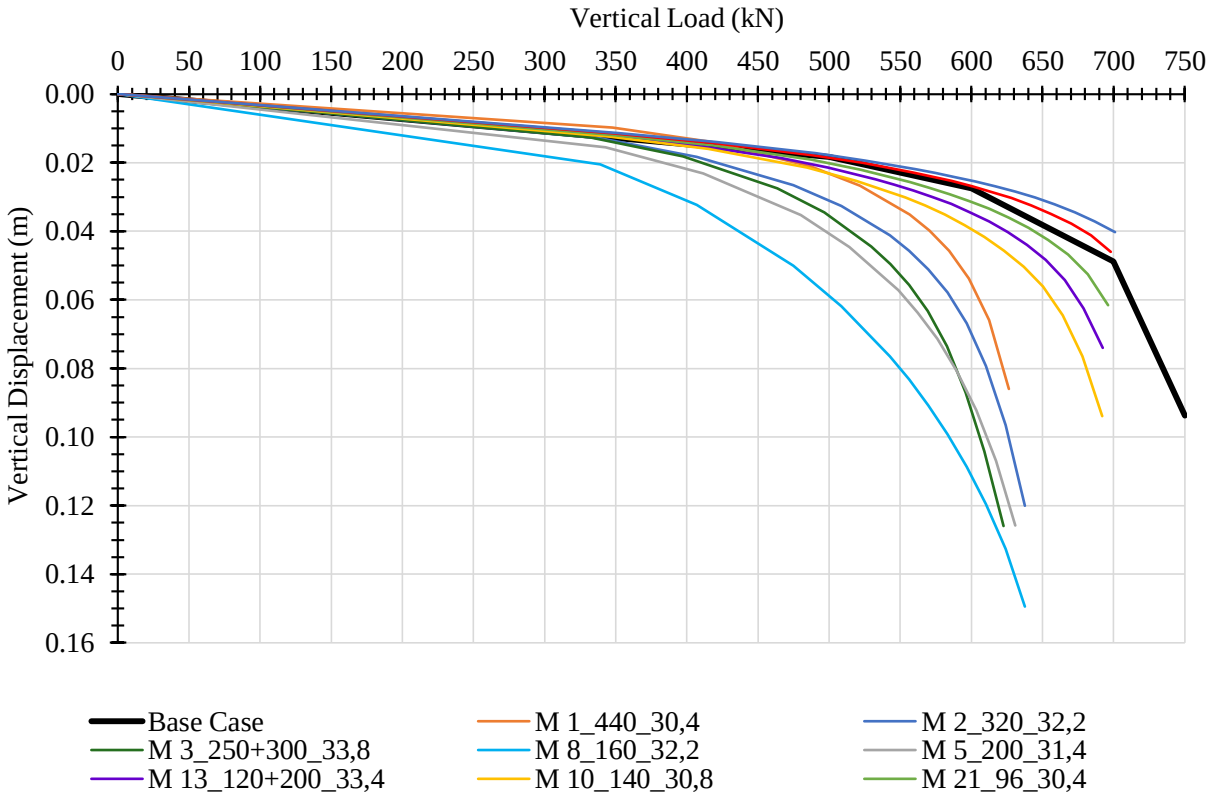

Figure 4.5 – Load *vs* vertical displacement (point A) curves to the first approach models

However, some models do not present the expected behaviour, deserving a special attention, i.e., *M 1_440_30,4* and *M 8_160_32,2*.

By doing a detailed review on the model *M 1_440_30,4* it is clear that during the elastic phase it presents lower displacements when compared to the base case, appearing to be better solution. But when it comes to the plasticity behaviour, its displacements increase overcoming the base case solution.

Bearing this in mind, 2D plane strain analyses were carried out representing the base case and the models *M 1_440_30,4* and *M 8_160_32,2* in order to understand why the first one presents less displacements than solutions with smaller perforations. Figure 4.6 presents the load *vs* vertical displacement curves, measured in the point with the largest settlements of each foundation. It can be seen that the perforated mudmats seem to have the same behaviour.

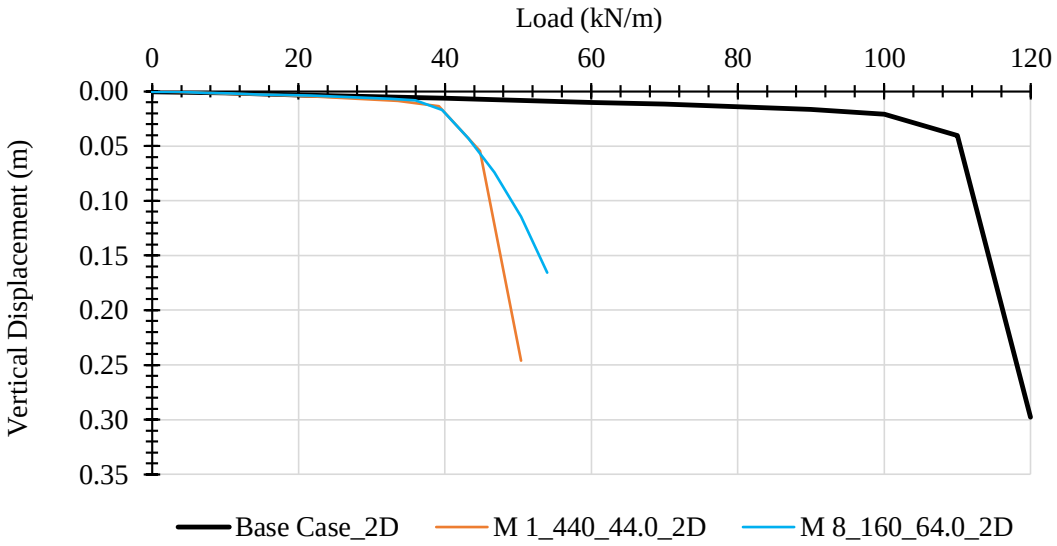

Figure 4.6 – Vertical displacements in the point with the largest vertical displacements in each model

On the other hand, when comparing the settlements bellow the foundations for the same applied load, shown in Figure 4.7, it is observed that in the model *M 1_440_44,0_2D*, point A tends to present less displacements than the other points of the foundation, as for the 3D model *M 1_440_30,4*. Figure 4.7 also shows that model *M 8_160_64,0_2D* presents an uniform settlement while model *M 1_440_44,0_2D* bends, presenting larger displacements on the edges. Thus, it can be concluded that foundations with higher number of holes tend to have more uniform settlements.

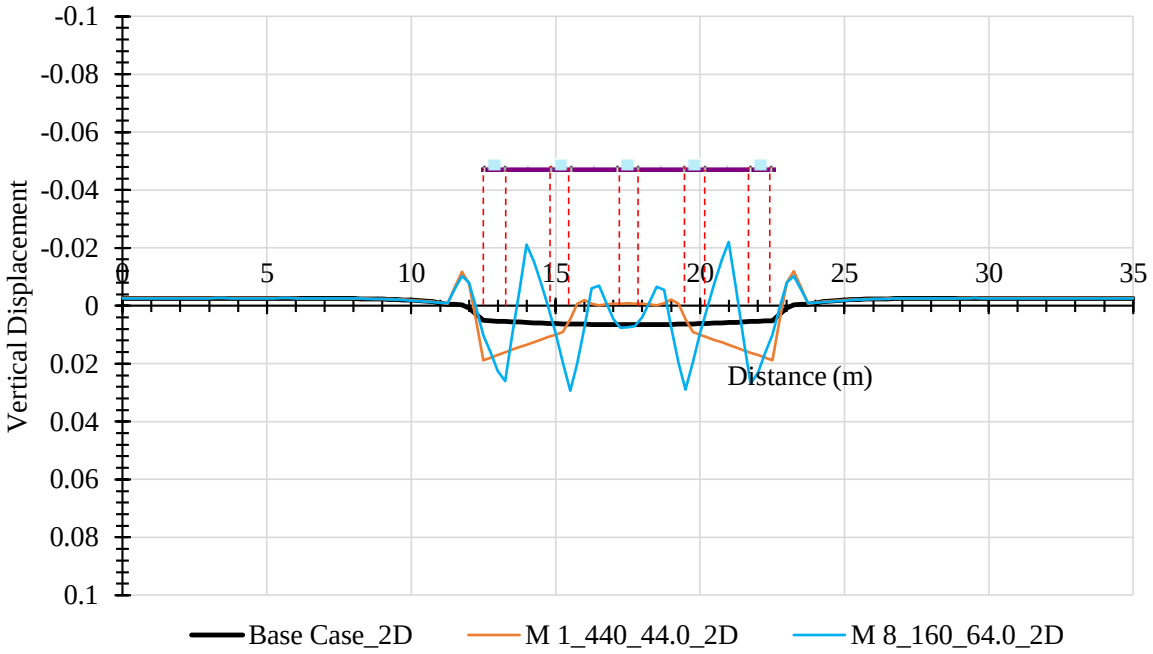

Figure 4.7 – Vertical displacements in the 2D models for 40 kN/m of vertical load

Contrary to what would be expected, although the model *M 8_160_32,2* has its holes distributed uniformly in the mudmat area, it presents higher displacements than models with more and smaller holes. This fact can be explained by the "grillage" effect created with the perforation, i.e. the framework of steel beams, as simplified in Figure 4.8.

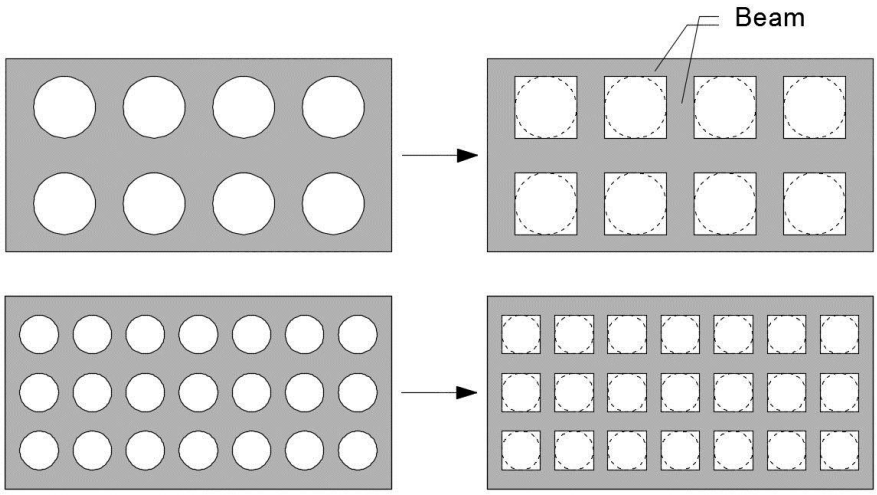

Figure 4.8 – Illustration of the effect of grillage created by the holes

It can be observed by comparing the results for other models that the displacement values tend to decrease as this "grillage" become denser (with more perforations and hence with thinner beams).

It can also be explained by the stress relieve that happens in non-loaded areas. Below each beam element it is created a pressure bulb. Taking into account that as the bulbs get closer, the stresses

between them increase, the respective behaviour of the perforated mudmat becomes closer to a solid one, as shown in Figure 4.9.

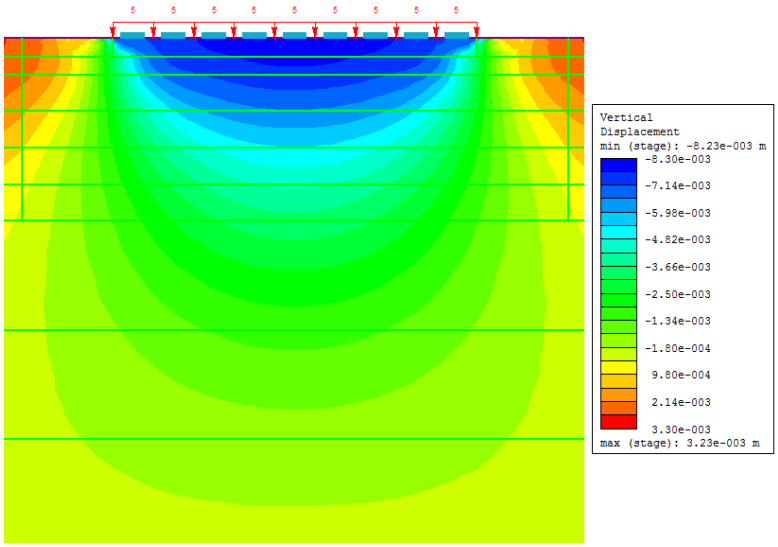

a)

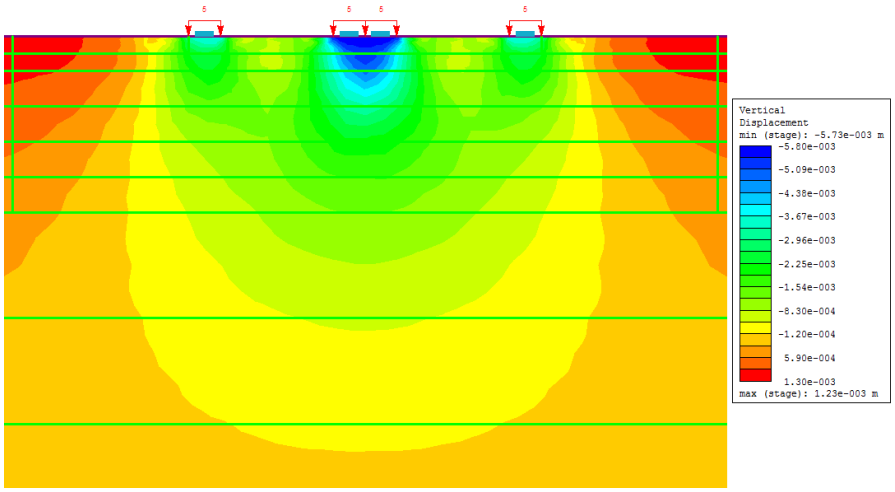

b)

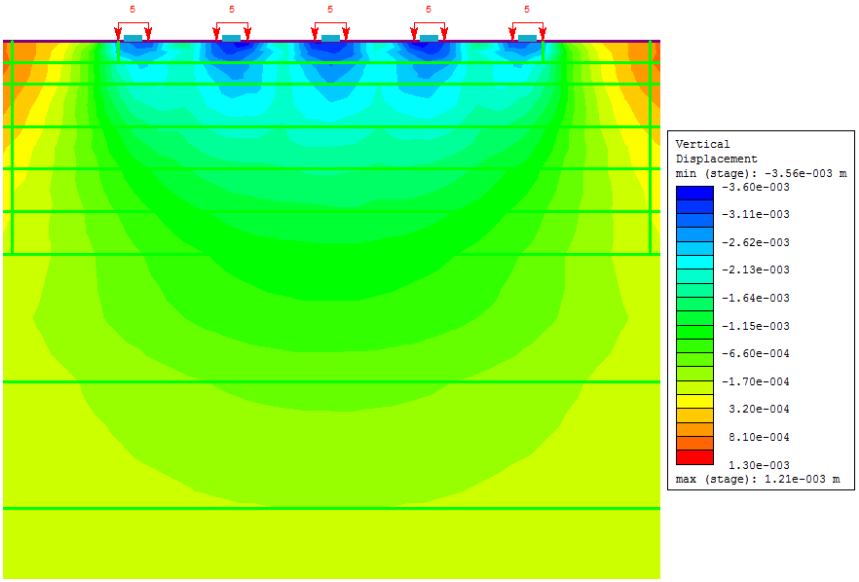

c)

Figure 4.9 – Vertical displacements diagram, obtained through 2D analyses, to the same stress (5 kPa), for: a) base case model; b) model *M 2_360_64.0_2D* and c) model *M 8_160_64.0_2D*

Focusing on the closer curves to the base case, it can be noted that those cases correspond to models with uniform holes' arrangements; with exception to the model *M 13_120+200_33,4*, which, although has a higher perforation ratio, shows less displacements than model *M10_140_30,8*. This fact can be once again explained by the fact that the mudmat behaves like two foundations in parallel, as in the model *M 1_440_30,4*, with the difference that these two small foundations are perforated instead of being completely solid.

However, when compared with model *M 1_440_30,4*, the model *M 13_120+200_33,4*, with an higher perforation ratio presents less displacements. This is because it has a smaller central perforation and larger foundations side by side, distributing the stresses.

Considering the above conclusions and taking into account the consistent behaviour when compared with the base case model, the subsequent studies were based exclusively on the following four models0: *M 10_140_30,8*; *M 21_96_30,4*; *M 50_62_30,2* and *M 90_46_29,9*.

4.3 Influence of Holes' Shape

In order to determine the influence of holes' shape, the four model referred above were tested maintaining the same number of holes and a similar perforation ratio, but square holes. This analysis was conducted with a similar mesh keeping the same node number.

Figure 4.10 presents the load *vs* vertical displacement curves. The models with square holes can be distinguished by the *"sq"* included in their nomenclature. And the number before these acronym give the side length of the square perforation, i.e. the name *M 50_55sq_30,3* means that the model has 50 perforations, with a side of 55 cm and 30,3% of perforation ratio.

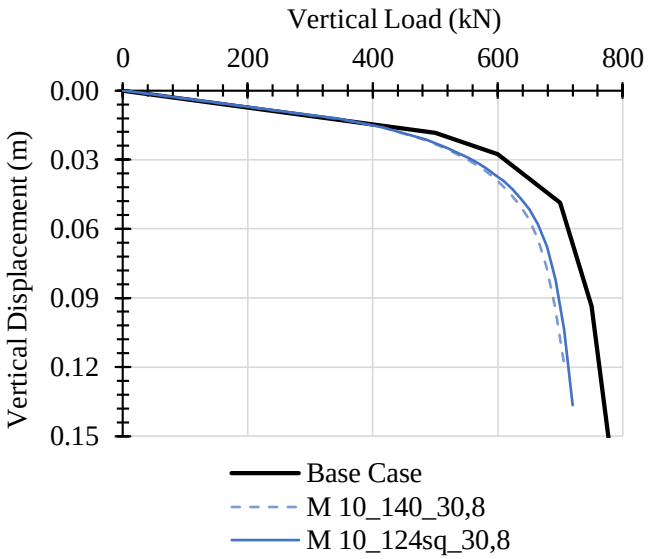

a)

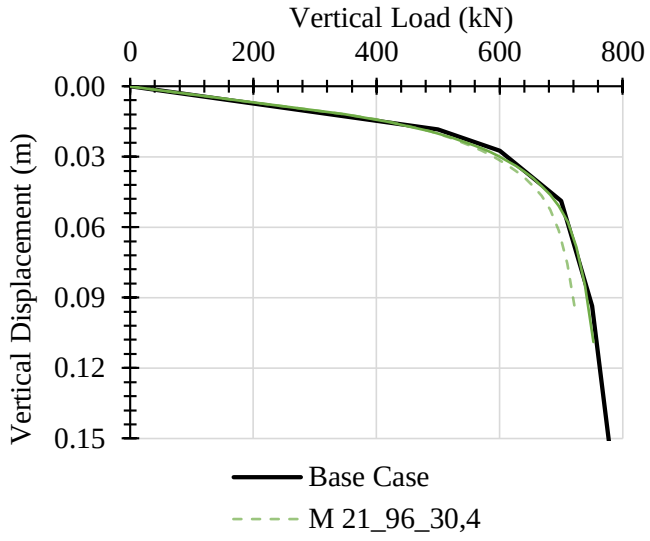

b)

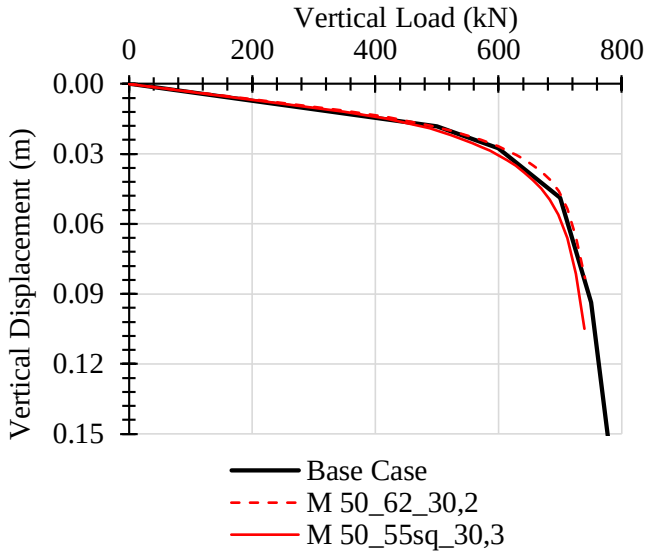

c)

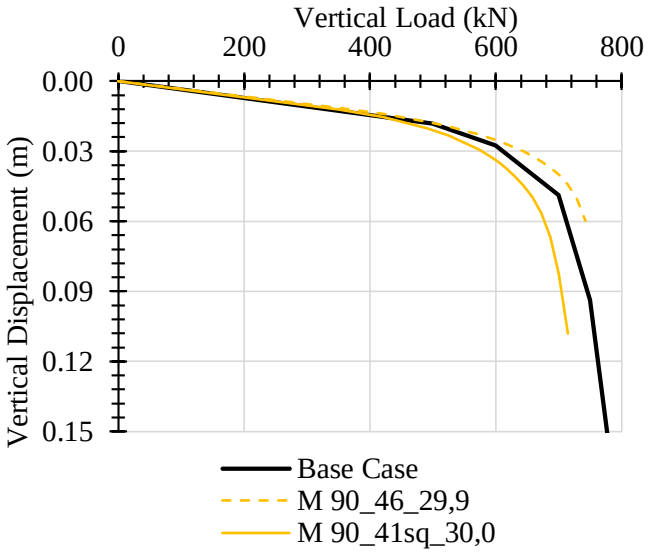

d)

Figure 4.10 - Vertical displacement, on point A, of perforated mudmats with circular and square holes: a) 10 perforations; b) 21 perforations; c) 50 perforations and d) 90 perforations

The curves present an almost imperceptible difference between them. It may be concluded that the holes' shape has a negligible influence in the foundation behaviour in terms of bearing capacity. Note that the curves of the model with 90 perforations do not show a complete agreement with each other. As will be seen, during the different analyses this was a continuous issue.

On the other hand, in terms of the structural behaviour, when using square holes, the local stresses tend to accumulate on its perforation corners, as shown in Figure 4.11, leading to

cracking in those areas or other structural problems. Thus, a square holes solution requires additional structural analysis, to assess the behaviour during installation and structure's design life.

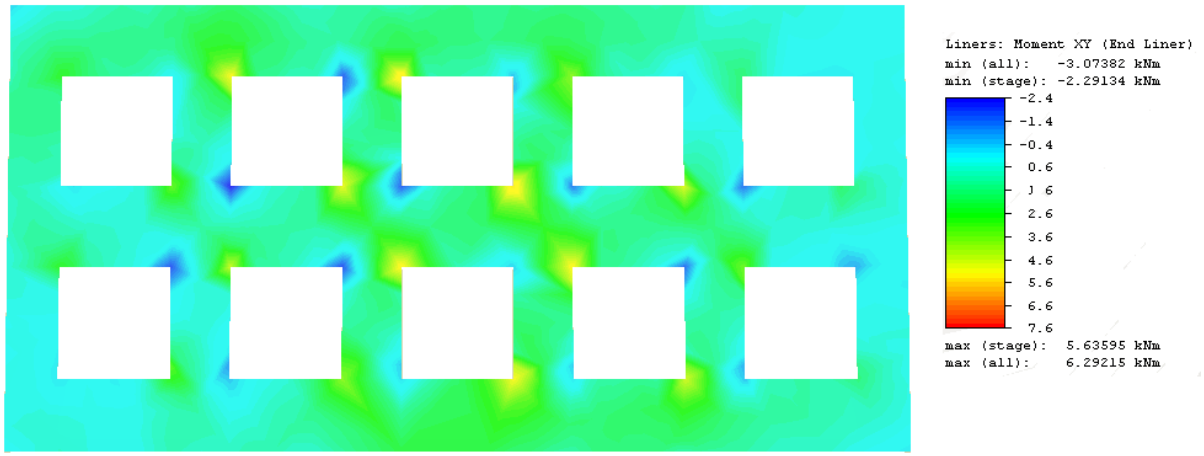

Figure 4.11 - Moment XY in model *M 10_124sq_30,8* at failure

4.4 Influence of Perforation Ratio

Aiming to assess the influence of the perforation ratio on the mudmat's bearing capacity, the models *M 10_140_30,8*; *M 21_96_30,4*; *M 50_62_30,2* and *M 90_46_29,9* were analysed varying the holes diameter, and hence the perforation ratio. Once more, this analysis corresponds to varying the width of each element that composes the grillage and observe how the load *vs* vertical displacement curve is influenced.

The load *vs* vertical displacement curves related to each model are shown on Figure 4.12 to Figure 4.15.

By getting a closer look at the results for the model with 10 perforations in a 50 meter squared mudmat, in Figure 4.12, it can be seen that, although this solution presents similar displacements to the base case, the perforation still has an important impact in its capacity. A perforation ratio of about 20% increases the settlements in less than 1 centimetre before failure in proportion with the base case. However, the impact become more perceptible when the perforation ratio increases. When the perforation ratio corresponds to 30% or a higher value, the difference between the base case and the failure happens for a smaller load. Thus, it can be concluded that the perforation diameter as a direct impact on the capacity of the foundation.

Regarding the Figure 4.13, it is possible to verify that although the perforation ratio has an impact in the vertical displacement, and hence in capacity, the 20% and 30% of perforation cases present the same behaviour. Above this ratio the settlements increase and the curves diverge from the base case behaviour.

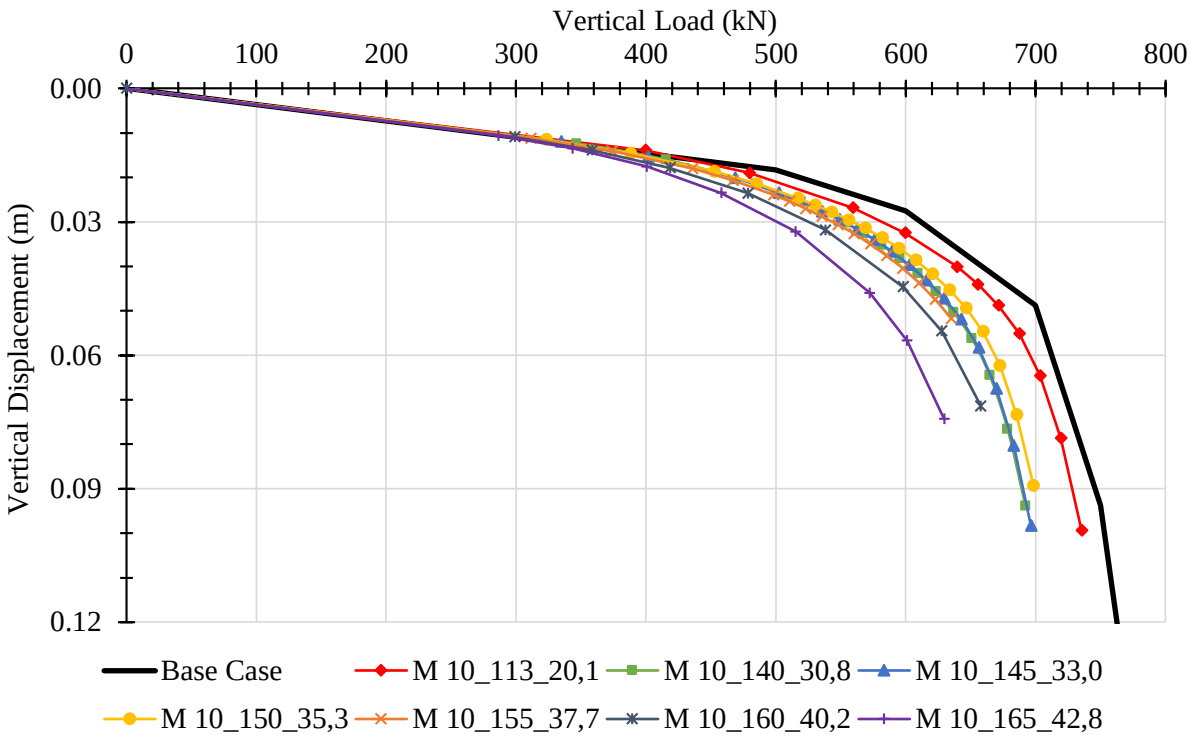

Figure 4.12 – Load *vs* vertical displacement curves for a model with 10 perforations

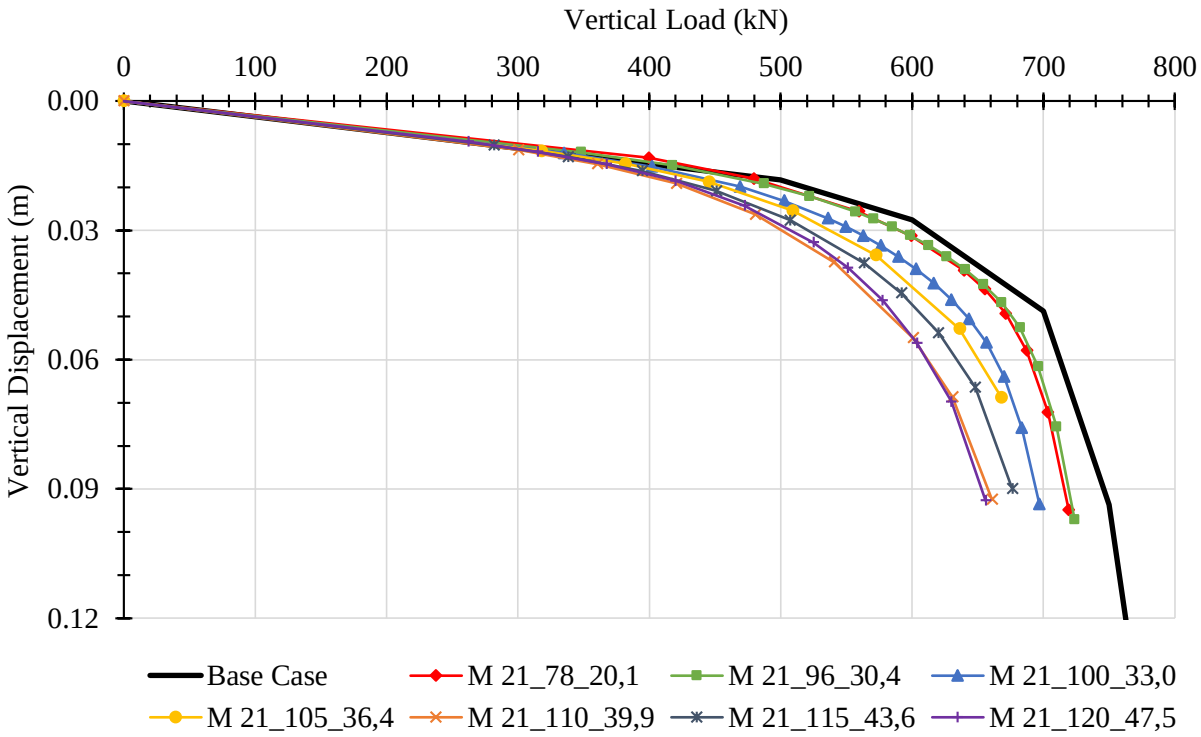

Figure 4.13 - Load *vs* vertical displacement curves for a model with 21 perforations

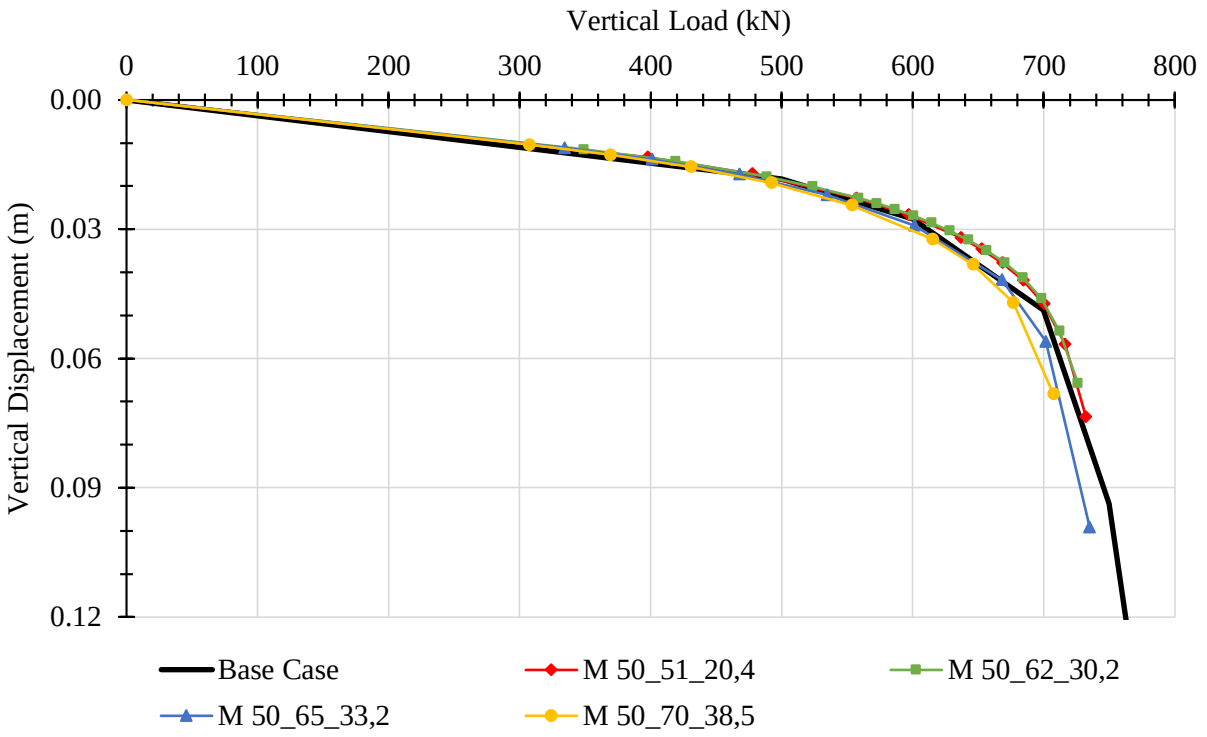

Figure 4.14 - Load *vs* vertical displacement curves for a model with 50 perforations

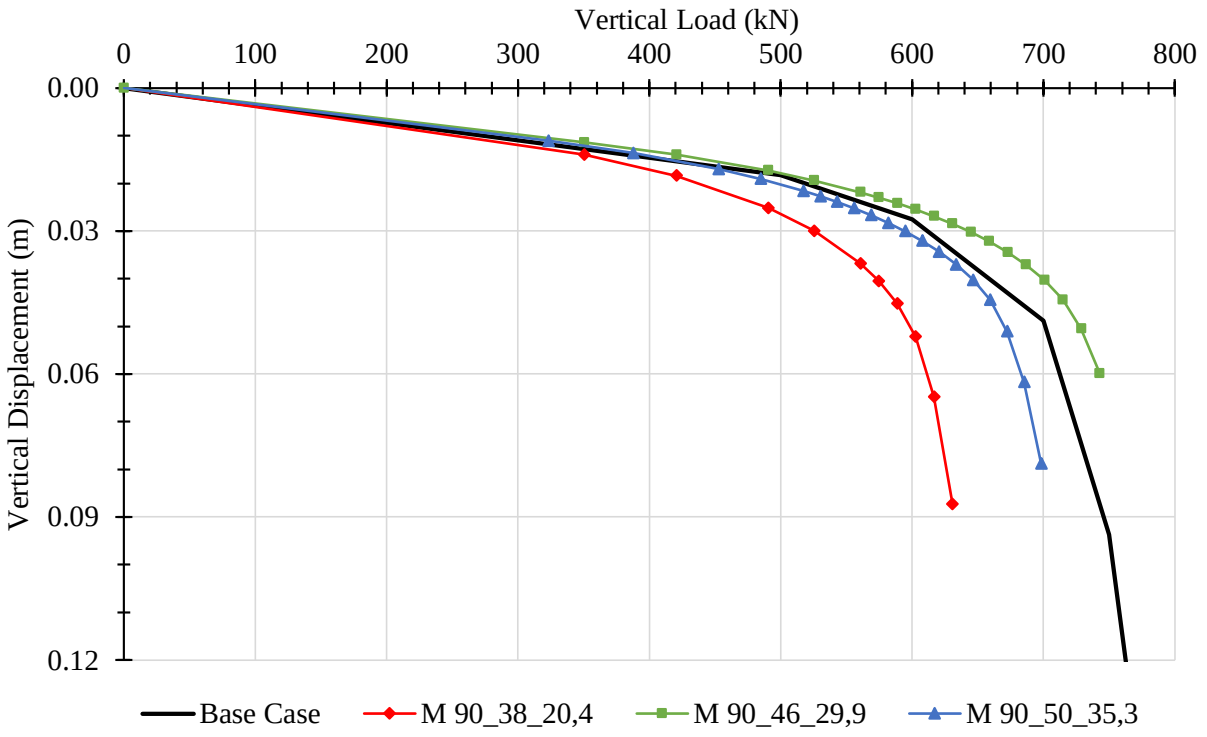

Figure 4.15 - Load *vs* vertical displacement curves for a model with 90 perforations

Observing the Figure 4.14, regarding the model with 50 perforations, it can be seen that this model represents almost perfectly the base case behaviour until 30% of perforation ratio. Above this value, the vertical displacement increases. However, the difference between this model and the base case is very small. Note that for a perforation ratio of 38,5% this difference is under 1 cm.

Concerning in a mudmat with 90 holes, it is difficult to establish a trend with the increase of the perforation ratio, as shown in Figure 4.15. The results either have higher displacements than the base case for a smaller ratio or show less settlements for higher perforations. These results can be related with the influence of the mesh, explained in section 3.2.4 of the previous chapter. The thin vertical mesh elements at the surface and shallow depths lead to inconsistencies.

By directly comparing the four models above for the same perforation ratio it is perceptible the grillage shape, i.e. increasing the number of holes increases de number of the grillage's elements and decreases each element width. Thus, it is possible to conclude that the model with 50 perforation is the model which better adjusts to the base case.

Regarding the curves inherent to 30% perforation ratio, it seems there is a trend to improve the behaviour when increasing the number of elements in the grillage and reducing its width. However, observing the 20% curves, the trend seems continue but have an exception for model *M 90_46_29,9*. This model presents less displacements than the base case for 30% of perforation, but higher values for 20% of perforation. As seen previously, this model revealed some issues that are the cause for the inconsistency in the results.

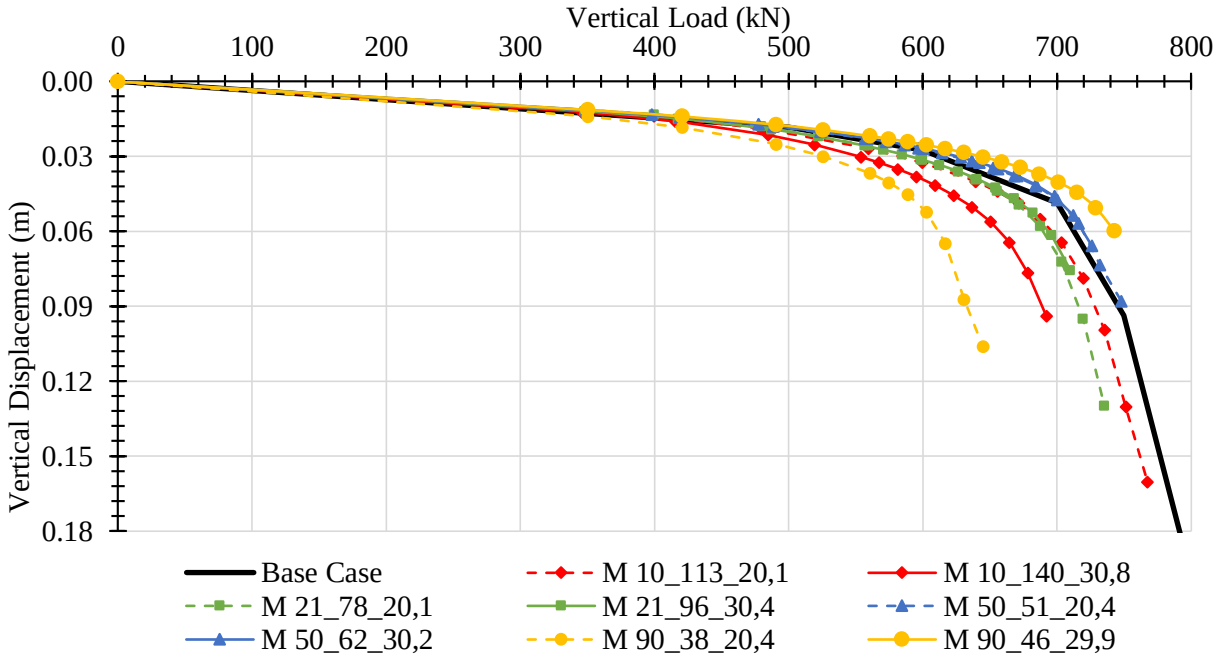

Figure 4.16 – Comparison between models with 10, 21, 50 and 90 holes for approximately 20% and 30% of perforation

4.5 Perforated Mudmat Behaviour under Combined Loading

Once installed on the seabed, the structures are subjected not only to vertical loading, but there are also horizontal forces acting leading to overturning or torsion moments. For this reason it is important to analyse the behaviour of a perforated mudmat under combined loading. This part of the study also includes the foundation behaviour when improved with structural skirts.

Considering that the model *M 50_62_30,2* was the model that presented the better adjustment to the base case, the forward studies were based exclusively on it.

4.5.1 Models without Skirts

Firstly, it was analysed the influence of the vertical loading acting simultaneously with the horizontal force in X direction at the mud level or the Y moment, separately.

The influence of the horizontal loading was assessed in two ways: applying a constant horizontal force and an increasing vertical loading and vice-versa. Comparing these cases in which it was applied a constant horizontal force of 50 kN and increased the vertical loading with the same models without horizontal loading applied, as shown in Figure 4.17, it can be clearly noticed that having an horizontal force applied has a higher influence in a perforated mudmat than in non-perforated one. However, the model *M 50_62_30,2* presents a different behaviour than the base case, in contrast to the verified in the analyses above.

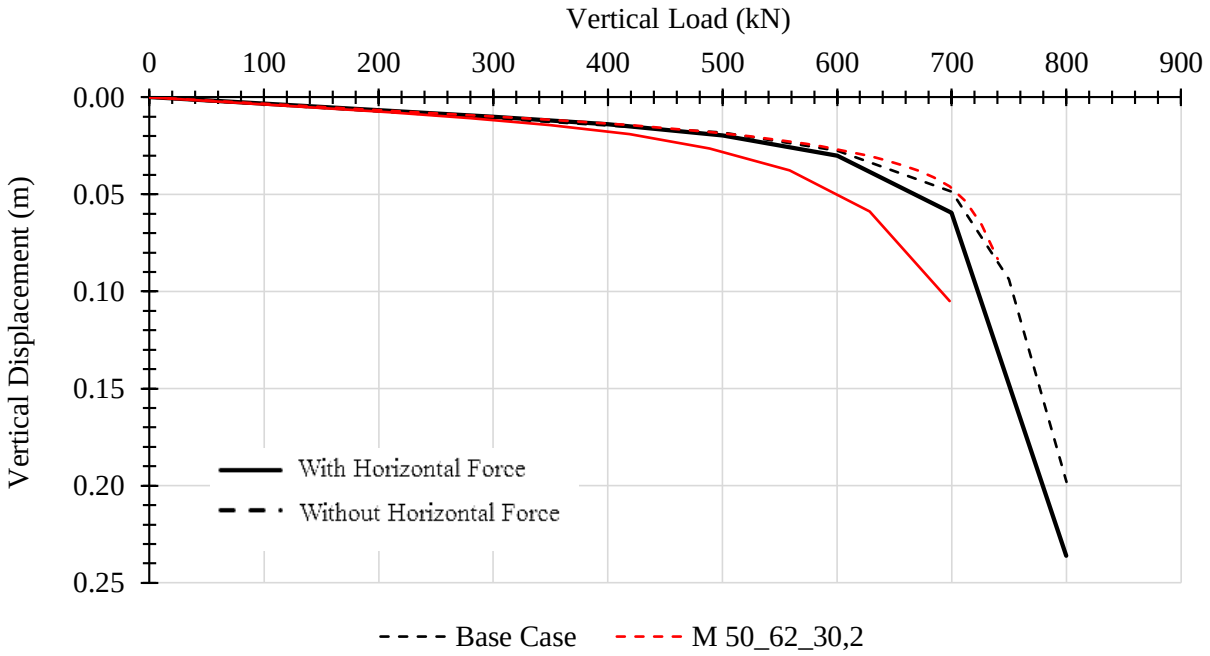

Figure 4.17 – Vertical displacements of *Base Case* and *M 50_62_30,2* with and without horizontal loading applied, in point A

Figure 4.18 shows an estimate of the interaction diagram between the vertical and horizontal loads, to the base case and the model *M 50_62_30,2*. Once again, the model with 50 perforations presents a similar behaviour to base case. However, in presence of horizontal load it tends to differ the base case behaviour.

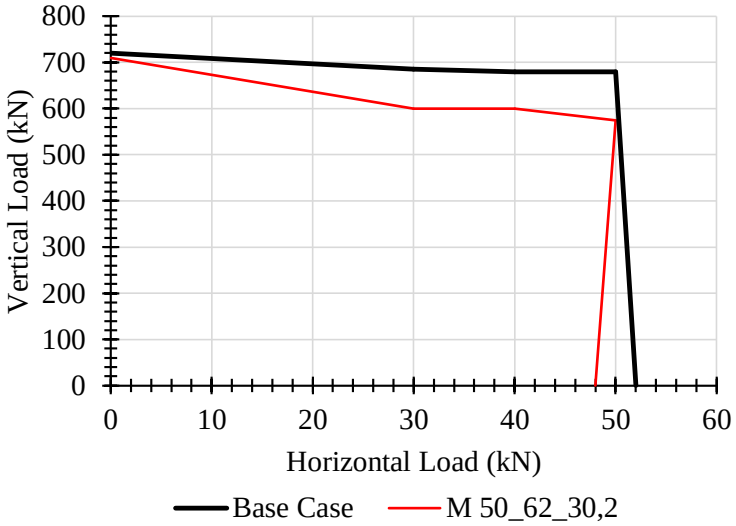

Figure 4.18 – Interaction diagrams for Base Case and *M 50_62_30,2* model

Compared with the diagram in Figure 2.5, the tendency of the vertical load to decrease with the increase of the horizontal is not clearly defined, nor the vertical envelope for sliding failure. These facts may be explained by several reasons: the chosen methods to determine the load at failure; their precision or the small number of points used to draw the envelope.

Figure 4.19 presents the horizontal displacement in X direction in function of the horizontal load for the models considering a simultaneously constant vertical loading equivalent to 600 kN. It is verified that the influence of the horizontal force becomes more perceptible for values higher than 40 kN. This fact can be explained by the area in contact with the soil which is smaller in the perforated mudmat whereas in the base case, leading to loss of adhesion to lower forces.

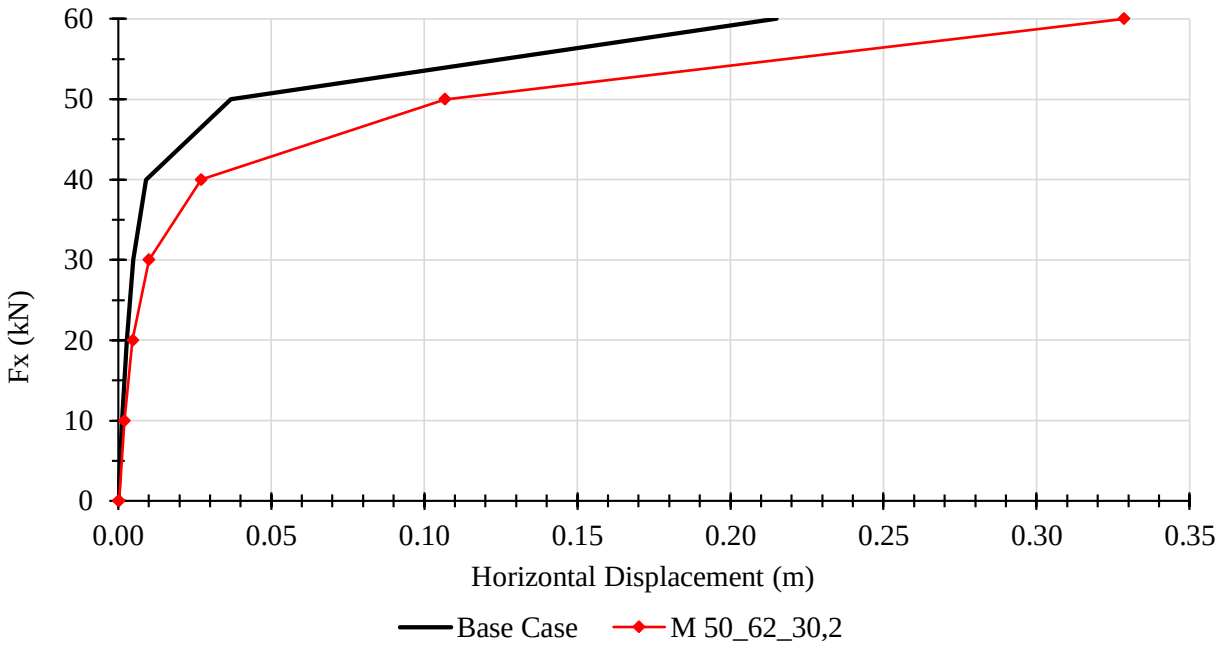

Figure 4.19 – Horizontal displacement curves, measured in point A, when mudmat are subjected to an uniform vertical loading equivalent to 600 kN and an increasing horizontal force in X direction

The Figure 4.20 presents the results for the results regarding the influence of having a moment around the Y axis applied simultaneously with a constant uniform vertical loading equivalent to 600 kN.

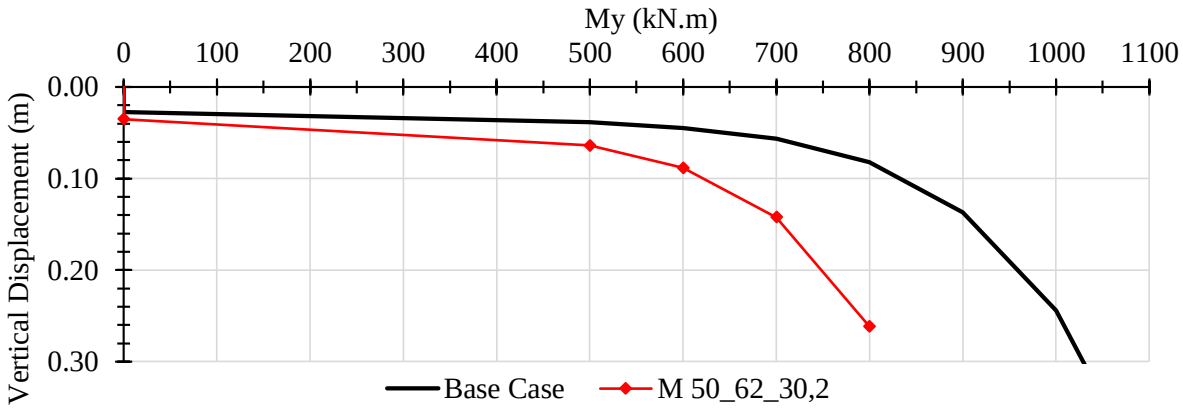

Figure 4.20 – Vertical displacement, in point A, in function of the moment around the Y axis when applied simultaneously with a constant vertical load

Taking into account the above figures and considering the previous analyses, it can be affirmed that perforation has stronger influence in mudmats subjected to combined loading.

4.5.2 With Skirts

In order to reverse the effect of perforation, skirts were added on the mudmat periphery providing an additional support, as seen in Figure 4.21. The skirts were simulated using vertical thin elements with 1 metre length (*d*), since it is usual to consider a ratio of *d/B* of 0,2 for subsea mudmats, with the same steel properties with a smaller thickness. Due to the soil properties being very low, no interface elements were considered.

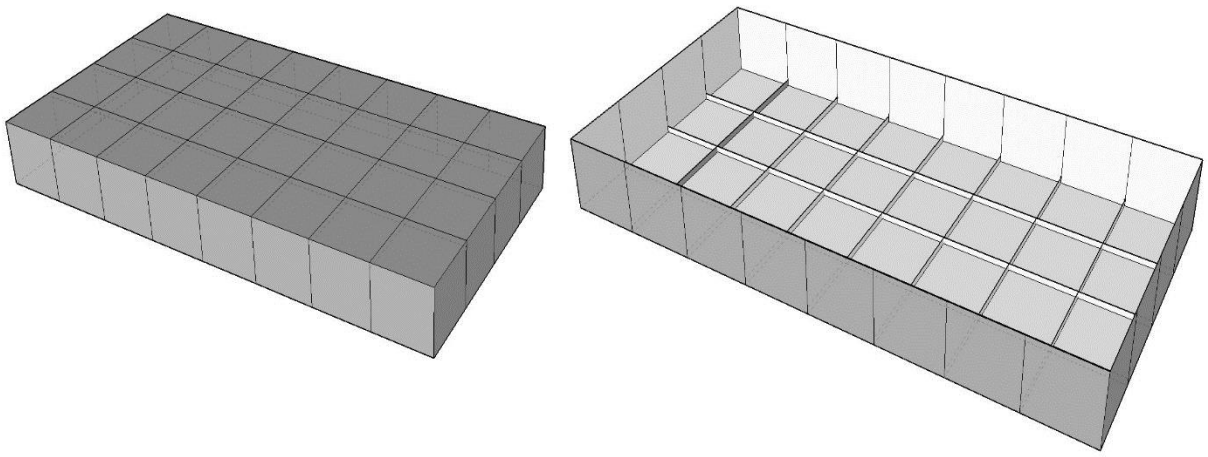

Figure 4.21 – Illustration of the added skirts

Thus, the three last analyses above were repeated adding skirts and the results are compared in Figure 4.22, Figure 4.23 and Figure 4.24.

The figures show that when skirts are added the mudmat behaviour improves, both in terms of vertical and horizontal displacements.

This allows to conclude that the loss of capacity that happens by adding perforations in mudmats can be balanced by adding skirts. In other words, it can be said that for mudmats with skirts the effect of perforation is almost negligible.

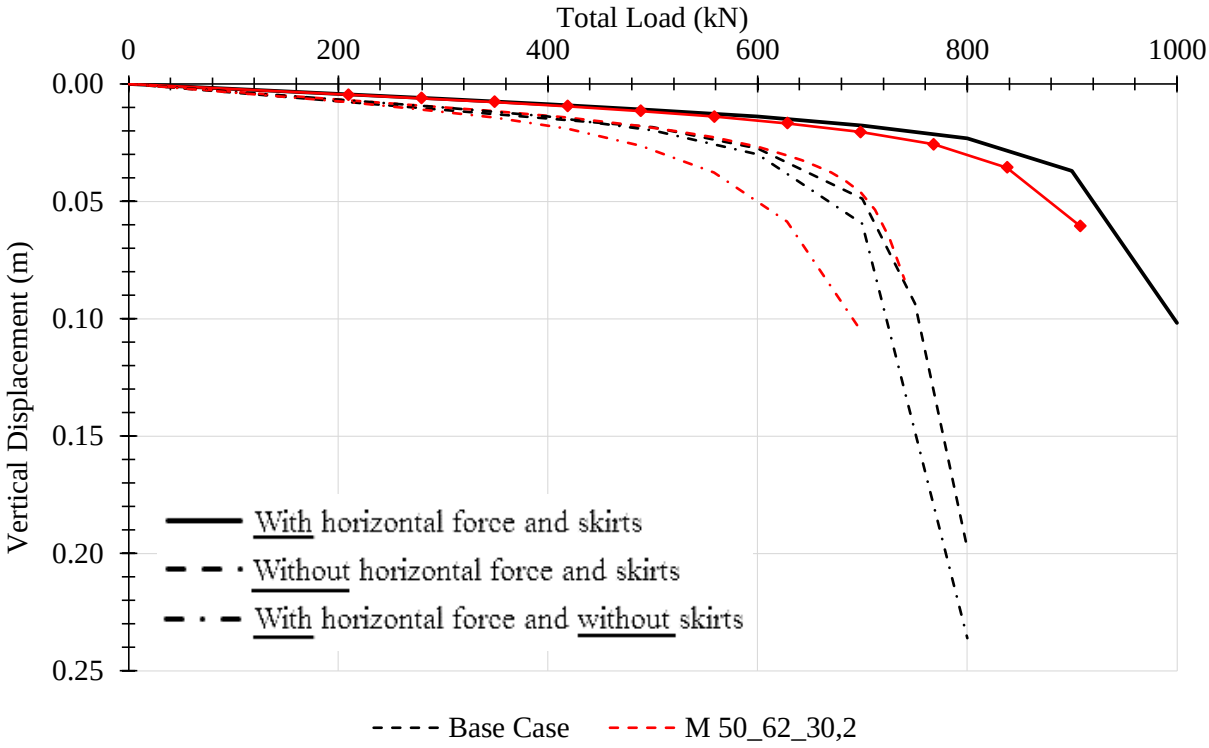

Figure 4.22 - Vertical displacements, in point A, of *Base Case* and *M 50_62_30,2* with and without horizontal loading applied, with and without skirts

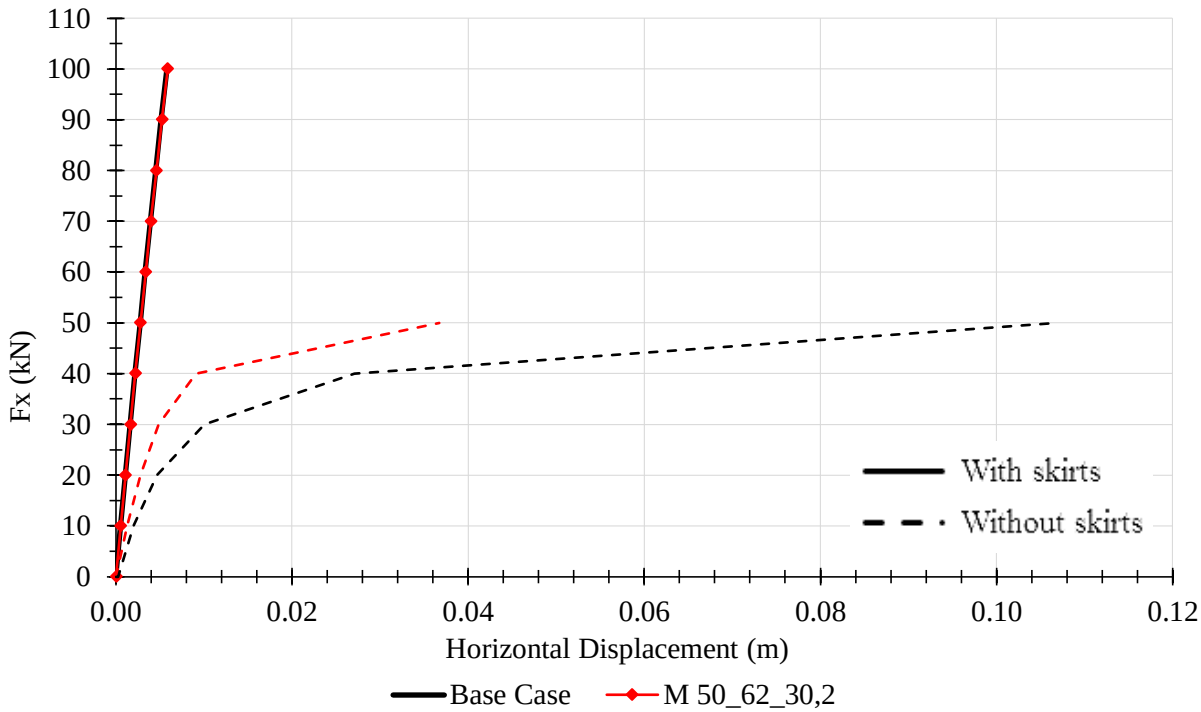

Figure 4.23 - Horizontal displacement curves, measured in point A, when mudmat are subjected to an uniform vertical loading equivalent to 600 kN and an increasing horizontal force in X direction, for mudmats with and without skirts

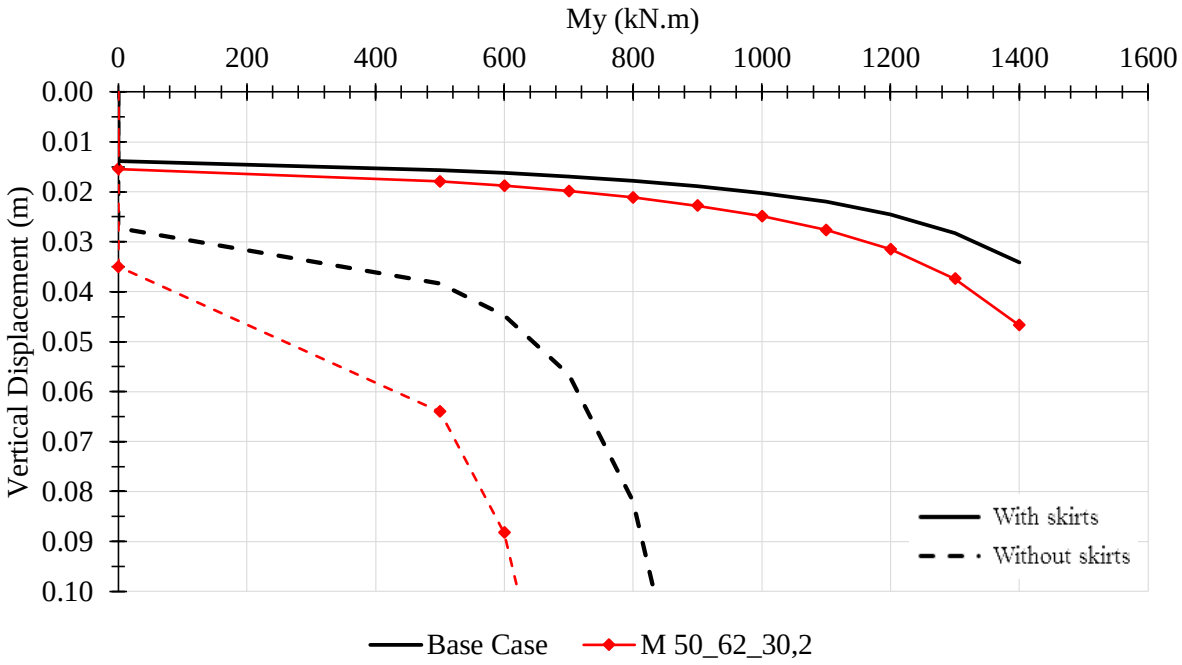

Figure 4.24 - Vertical displacement in point A in function of the moment around the Y axis when applied simultaneously with a constant vertical load, for mudmats with and without skirts

Finally, to complement the previous analyses in the present subchapter, it was analysed the mudmat behaviour under a more complex load scenario: vertical and horizontal forces and moment in Y direction. The applied loading is presented in Table 4.2 and the respective vertical displacements are shown in Figure 4.25.

Table 4.2 – Applied loading

Fx (kN)	*0*	*50*	*50*	*60*	*80*	*80*
Fz (kN)	*0*	*300*	*400*	*500*	*600*	*700*
My (kN.m)	*0*	*0*	*500*	*1000*	*1400*	*1600*

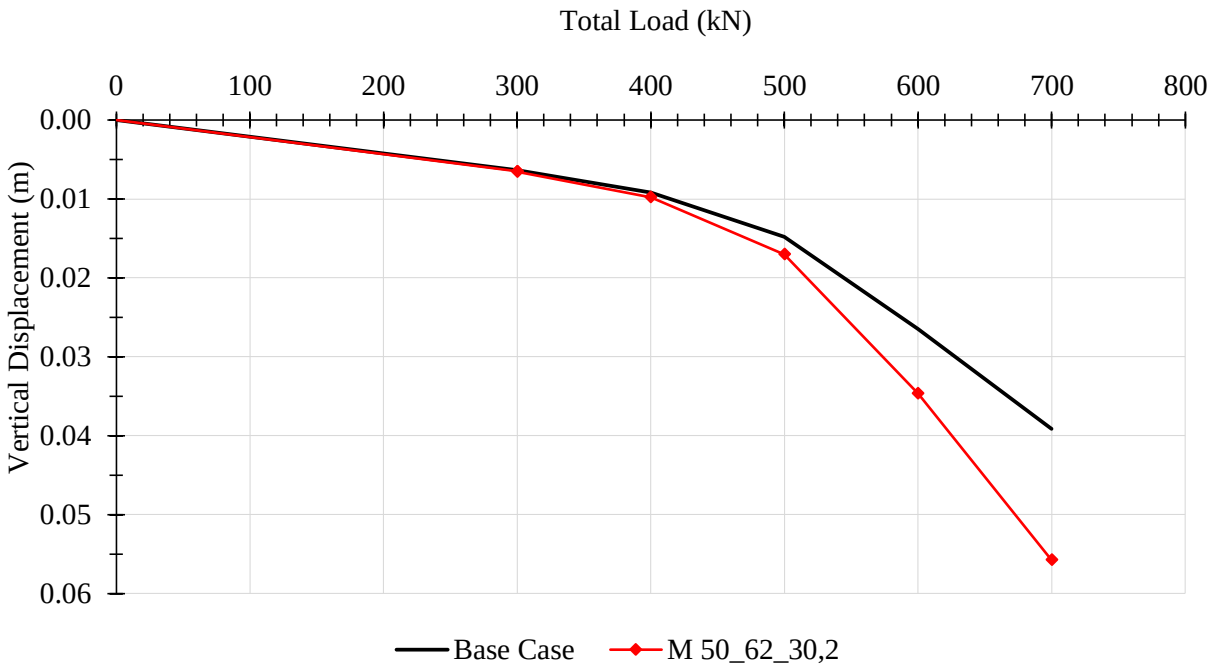

Figure 4.25 – Vertical displacements in point A for mudmats under combined loading

In addition to the analyses made previously in this chapter, the figure above shows once more the reliability of the model M 50_62_30,2 to the base case.

5 CONCLUSIONS AND PROPOSALS FOR FUTURE WORK

5.1 Conclusions

The aim of the present dissertation is to assess the perforations effect in the foundations bearing capacity, mainly installed on soils with very low shear strength profiles. The study focus mainly on the influence of the perforation ratio, taking also into account the influence of the holes' arrangement, shape and number. This research was carried out using FE analyses through the use of the software RS3.

Regarding the holes' arrangement it was concluded that uniform arrangements lead to less vertical displacements, since the mudmat acts as a uniform grillage, distributing the load uniformly to the soil. Also the number of holes has an influence on the mudmat behaviour, reducing its displacements as the number of perforations increases since the grillage becomes denser (with more and smaller holes) allowing, in consequence of the uniform distribution of the stress, the mudmat to behave like it was solid. Although, the mudmat behaviour improves when using a large number of small perforations, the model presented some inconsistencies on the mesh, and for that reason, it is not possible to have a valid conclusion.

The above conclusions are summarized in Table 5.1. The reduction in bearing capacity was calculated based on the ultimate load. Each model was compared with the base case.

Table 5.1 – Bearing capacity reduction correspondent to the holes' arrangement effect

Model	***Reduction***
M 1_440_30,4	18%
M 2_320_32,2	17%
M 3_250+300_33,8	19%
M 8_160_32,2	19%
M 5_200_31,4	18%
M 13_120+200_33,4	7%
M 10_140_30,8	8%
M 21_96_30,4	5%
M 50_62_30,2	3%
M 90_46_29,9	3%

Concerning the perforation ratio, the research, as presented in section 4.4, shows a good performance for models with 20% and 30% of perforated area and in some cases (for example model with 50 perforations), this value can be increased without affecting significantly the foundation bearing capacity. Even so, the maximum feasible value of perforation to use is determined in function of the number of perforations and their arrangement in the mudmat surface. Table 5.2 presents a summary of the influence of the perforation ratio in terms of the bearing capacity reduction. The values were calculated through the same process as those shown in the previous table.

Table 5.2 – Bearing capacity reduction correspondent to the perforation ratio effect

Model	***Reduction***	***Model***	***Reduction***	***Model***	***Reduction***	***Model***	***Reduction***
M 10_113_20,1	3%	*M 21_78_20,1*	5%	*M 50_51_20,4*	3%	*M 90_38_20,4*	18%
M 10_140_30,8	8%	*M 21_96_30,4*	5%	*M 50_62_30,2*	3%	*M 90_46_29,9*	7%
M 10_145_33,0	8%	*M 21_100_33,0*	8%	*M 50_65_33,2*	7%	*M 90_50_35,3*	8%
M 10_150_35,3	8%	*M 21_105_36,4*	9%	*M 50_70_38,5*	7%		
M 10_155_37,7	-	*M 21_110_39,9*	15%				
M 10_160_40,2	11%	*M 21_115_43,6*	13%				
M 10_165_42,8	13%	*M 21_120_47,5*	15%				

In addition to the above conclusion, the effect of the perforation shape was also assessed. These analyses determined that there were no advantage on having square holes instead of round, as noted in the bearing reduction shown in Table 5.3. Since no major differences were found on the bearing capacity, stress concentrations were observed in the holes' corners.

Table 5.3 – Bearing capacity reduction correspondent to the holes' shape effect

Model	***Reduction***	***Model***	***Reduction***
M 10_140_30,8	8%	*M 10_124sq_30,8*	6%
M 21_96_30,4	5%	*M 21_85sq_30,3*	1%
M 50_62_30,2	3%	*M 50_55sq_30,3*	4%
M 90_46_29,9	3%	*M 90_41sq_30,0*	7%

Finally, the analysis of the mudmat behaviour under combined loading, either with or without skirts, confirmed that the model *M 50_62_30,2* presents an excellent adjustment to the solid mudmat behaviour. Moreover, it determined that the skirts represent an important solution to provide additional capacity to shallow foundations, in this case, to perforated mudmats.

To summarize, and in agreement with White et. al. (2005), the results of the present dissertation allow to affirm that an optimal design to perforated foundations correspond to a large number of holes uniformly distributed in the mudmat area, and adding skirts.

5.2 Proposals for future work

Aiming to additional information the work developed during this dissertation, assessing of the behaviour of perforated mudmats in different conditions, some proposals for future works are suggested.

Regarding the geotechnical assessment, there are some information about perforated foundations that should be analysed, such as:

- Consolidation analyses, assessing the development of the undrained shear strength and analysing the bearing capacity over time;
- Test the impact of the mudmat area combined with the same perforation ratio;
- Analyse the effect of perforation on foundation bearing capacity in other types of soils.

In addition to these proposals, it would be also pertinent and interesting, since RS3 is a recent software for geotechnical application, to compare the results obtained with the ones using PLAXIS or ABAQUS, two of the most used software by Geotechnical companies. This comparison would strengthen the RS3 accuracy to reality, and reduce any minor error.

Outside the geotechnical context and since the main objective of adding perforations in mudmats is to reduce the installation loads, it is also important to analyse the present models in terms of structural/hydrodynamic behaviour during installation and the structure design life.

REFERENCES

Alves, D. (2014). "Ensaios em modelos reduzidos de sapatas com reforços laterais". Master Dissertation, Civil Engineering Department, University of Coimbra, Coimbra, Portugal.

API RP 2A WSD (2005). "Recommended Practice for Planning, Design and Constructing Fixed Offshore Platforms – Working Stress Design". 21st ed., American Petroleum Institute, Washington, U.S.A.

API RP 2A LRFD (1997). "Recommended Practice for Planning, Design and Constructing Fixed Offshore Platforms – Load and Resistance Factor Design" 1st ed., Washington, U.S.A.

Atkinson, J. (2007). "The mechanics of soil and foundations". Taylor & Francis, Abingdon, Oxon, U.K.

Bell, R. W. (1991). "The analysis of offshore foundations subjected to combined loading". Master Dissertation, University of Oxford, Oxford, U.K.

Bienen, B., Gaudin, C., Cassidy, M. J., Rausch, L., Purwana, O. A. and Krisdani, H. (2012). Computers and Geotechnics, Vol. 45, pp. 127-139.

Bowles, J. E. (1996). "Foundation Analysis and Design". 5th Edition, McGraw-Hill, New York, U.S.A.

Cassidy, M. J., Randolph, M. F. and Byrne, B. W. (2007). "A plasticity model describing caisson behaviour in clay". Applied Ocean Research, Vol. 38, pp. 345-358.

Chen, R., Gaudin, C. and Cassidy, M. J. (2012). "Investigation of the vertical uplift capacity of deep water mudmats in clay". Canadian Geotechnical Journal, Vol. 49, pp. 853-865.

Dean, E. T. R. (2010). "Offshore Geotechnical Engineering". London, U.K.

DNV RP H103 (2011). "Recommended Practice for Modelling and Analysis of Marine Operations". Det Norske Veritas, Norway.

DNV CN 30.4 (1992). "Foundations". Det Norske Veritas, Norway.

Fagundes, D. F., Almeida, M. C. F., Almeida, M. S. S. and Rammah, K. I. (2012). "Physical modelling of offshore structures founded on sea bed". Proceedings of the 31st International Conference on Ocean, Offshore an Arctic Engineering, ASME, Rio de Janeiro, Brazil.

Feng, X., Gourvenec, S. and Randolph, M. F. (2014). "Optimal skirt spacing for subsea mudmats under loading in six degrees of freedom". Applied Ocean Research, Vol. 48, pp. 10-20.

Feng, X., Randolph, M. F., Gourvenec, S. and Wallerand, R. (2013). "Design approach for rectangular mudmats under fully three-dimensional loading". Géotechnique, Vol. 64, Issue 1, pp. 51-63.

Gourvenec, S., Randolph, M. F. and Kingsnorth, O. (2006). "Undrained bearing capacity of square and rectangular footings". International Journal of Geomechanics, May/June 2006, pp. 147-157.

Hu, Y. and Randolph, M. F. (1998). "Deep Penetration of shallow foundations on non-homogeneous soil". Soils and Foundations, Vol. 38, No. 1, pp. 241-246.

Hu, Y. and Randolph, M. F. (1998). "H-adaptive FE analysis of elasto-plastic non-homogeneous soil with large deformation". Computers and Geotechnics, Vol. 23, pp. 61-83.

Lunne, T., Andersen, K. H., Low, H. E., Randolph, M. F. and Sjursen, M. (2011). "Guidelines for offshore *in situ* testing and interpretation in deepwater soft clays". Canadian Geotechnics Journal, Vol. 48, pp. 543-556.

Martin, C. M. (1994). "Physical and numerical modelling of offshore foundations under combined loads". Doctoral Thesis, University of Oxford, Oxford, U.K.

Mccarron, William O. (2011). "Deepwater Foundations and Pipeline Geomechanics". J. Ross Publishing, U.S.A.

Plaxis: Material Models Manual (2015). Delft, Netherlands.

Pusadkar, S. S. and Bhatkar, T. (2013). "Behaviour of Raft Foundations with vertical skirts using Plaxis 2D". International Journal of Engineering Research and Development, Vol. 7, Issue 6, pp. 20-24.

Randolph, M. F. and Gourvenec, S. (2011). "Offshore Geotechnical Engineering". Spon Press, Abingdon, Oxon, U.K.

Rocscience@ (2016). https://www.rocscience.com/help/phase2/webhelp9/phase2.htm. RS2 online help, Rocscience official web site, Toronto, Canada.

Rocscience@ (2016). https://www.rocscience.com/help/RS3/webhelp/RS3.htm. RS3 online help, Rocscience official web site, Toronto, Canada.

Salgado, R., Lyamin, A. V., Sloan, S. W. and Yu, H. (2004). "Two- and three-dimensional bearing capacity of foundations in clay". Géotechnique, Vol. 54, No. 5, pp. 297-306.

Santa Maria, P. E. L. (1988). "Behaviour of footings for offshore structures under combined loads". Doctoral Thesis, University of Oxford, Oxford, U.K.

Silva, J. (2014). "Análise Numérica de Ensaios a 1G em modelos reduzidos de fundações diretas". Master Dissertation, Civil Engineering Department, University of Coimbra, Coimbra, Portugal.

Stelzer, R. and Hofstetter, G. (2005). "Adaptive finite element analysis of multi-phase problems in geotechnics". Computers and Geotechnics, Vol. 32, pp. 458-481.

TECH-FAB@ (2015). http://www.tech-fab.com/subsea-mudmat.html. Tech-Fab Custom & Production metal fabrications (official web site), Texas, U.S.A.

Terzaghi, Karl (1943). "Theoretical Soil Mechanics". John Wiley and Sons, Inc., New York, U.S.A.

White, D. J., Meconochie, A. J., Cheuk, C. Y. & Bolton, M. D. and Joray, D. & Springman, S. M. (2005). "An investigation into the vertical bearing capacity of perforated mudmats". Proceedings of the International Symposium on Frontiers in Offshore Geotechnics, ISFOG, Perth, Australia.

Zhou, H. and Randolph. M. F. (2006). "Large deformation analysis of suction caisson installation in clay". Canadian Geotechnics Journal, Vol. 43, pp. 1344-1357.